

# The Discovery and Optimization of a Novel Class of Potent, Selective, and Orally Bioavailable Anaplastic Lymphoma Kinase (ALK) Inhibitors with Potential Utility for the Treatment of Cancer

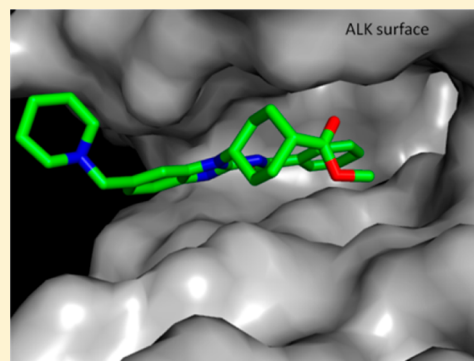
Richard T. Lewis,<sup>\*,†</sup> Christiane M. Bode,<sup>†</sup> Deborah M. Choquette,<sup>†</sup> Michele Potashman,<sup>†</sup> Karina Romero,<sup>†</sup> John C. Stellwagen,<sup>†</sup> Yohannes Teffera,<sup>†</sup> Earl Moore,<sup>†</sup> Douglas A. Whittington,<sup>†</sup> Hao Chen,<sup>†</sup> Linda F. Epstein,<sup>†</sup> Renee Emkey,<sup>†</sup> Paul S. Andrews,<sup>†</sup> Violeta L. Yu,<sup>†</sup> Douglas C. Saffran,<sup>†</sup> Man Xu,<sup>†</sup> Allison Drew,<sup>†</sup> Patricia Merkel,<sup>†</sup> Steven Szilvassy,<sup>‡</sup> and Rachael L. Brake<sup>†</sup>

<sup>†</sup>Amgen Inc., 360 Binney Street, Cambridge Massachusetts 02142, United States

<sup>‡</sup>Amgen Inc., One Amgen Center Drive, Thousand Oaks, California 91320, United States

## S Supporting Information

**ABSTRACT:** A class of 2-acyliminobenzimidazoles has been developed as potent and selective inhibitors of anaplastic lymphoma kinase (ALK). Structure based design facilitated the rapid development of structure–activity relationships (SAR) and the optimization of kinase selectivity. Introduction of an optimally placed polar substituent was key to solving issues of metabolic stability and led to the development of potent, selective, orally bioavailable ALK inhibitors. Compound **49** achieved substantial tumor regression in an NPM-ALK driven murine tumor xenograft model when dosed qd. Compounds **36** and **49** show favorable potency and PK characteristics in preclinical species indicative of suitability for further development.



## ■ INTRODUCTION

Anaplastic lymphoma kinase (ALK) is a receptor tyrosine kinase classified as belonging to the insulin receptor superfamily. Expressed at high levels prenatally, it is thought to play an important role in the development of the central nervous system. However, its expression is dramatically decreased in healthy adult tissues. Aberrant expression of full-length ALK occurs in neuroblastoma and is associated with increased gene copy number or activating point mutations.<sup>1</sup> Furthermore, chromosomal translocation or inversion of the ALK gene can lead to the generation of novel fusion-ALK proteins that possess constitutive kinase activity and contribute to oncogenic processes. The best validated of these include an ALK fusion protein with nucleophosmin (NPM-ALK), which has been characterized in a subset of anaplastic large-cell lymphomas<sup>2</sup> and an alternate gene splicing event pairing the ALK kinase domain with echinoderm microtubule-associated protein-like 4 (EML4-ALK), which provides the driving oncogene in a subset of non-small cell lung carcinomas (NSCLC).<sup>3</sup> A potent and selective inhibitor of the ALK kinase domain would have potential therapeutic utility in a range of cancers. Compound **3**, PF-02341066, now known as Crizotinib, afforded the first clinical validation of EML4-ALK as an oncology target and is now FDA approved as a first-line treatment for this patient population.<sup>4</sup> Reports of developing resistance to crizotinib have

provided added impetus to seek significantly more potent molecules with potential to treat refractory patients.<sup>5</sup>

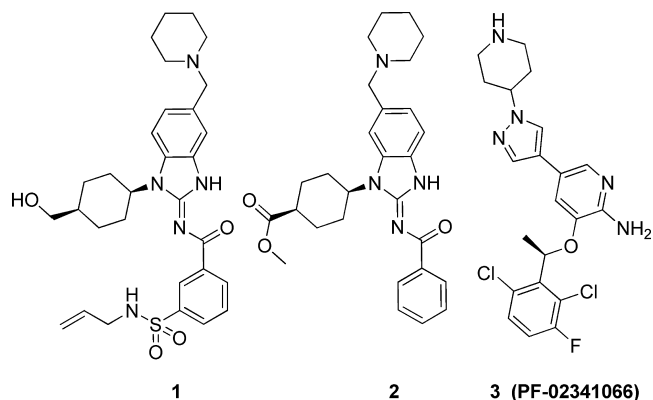
Identification of an ALK inhibitor with significant selectivity over the majority of the known kinome would be very desirable in order to capitalize on a key characteristic of ALK, namely a therapeutic target functionally expressed in a subset of cancers, which is seldom expressed in healthy adult tissue. In pursuit of this goal, enzymatic activity was routinely monitored against related tyrosine kinase family members SRC kinase, insulin-like growth factor receptor 1 (IGF1R), and the janus kinase (JAK) family<sup>6</sup> during the triage of hits from high-throughput screening (HTS) to identify selective leads and also in the subsequent lead optimization phase described herein. Selectivity ratios with respect to ALK enzyme potency are used in this account of the work; the IC<sub>50</sub> values against these off-target enzymes are reported in the Supporting Information (Table S3). IGF1R was used as a convenient enzymatic surrogate for the insulin receptor (INSR), against which a 100-fold selectivity margin was sought. Inhibition of ALK phosphorylation, measured by monitoring inhibition of ALK phosphorylation at Tyr1604 in a whole cell context (pALK cell), was used to assess cellular potency and was the principal driver of SAR. A functional cellular assay assessing the ability of compound to inhibit the in

Received: April 26, 2012

Published: June 26, 2012

in vitro proliferation of an NPM-ALK-driven cell line (Karpas-299) was also utilized.<sup>7</sup> Excellent correlation between compound potency as measured in the pALK cellular biochemical assay and the in vitro functional proliferation assay was observed. Consequently, the pALK cellular biochemical readout proved a reliable means to select at an early point in the screening cascade those compounds possessing good cellular penetration and hence of identifying compounds with a greater probability of achieving superior in vivo potency.

X-ray quality crystals of the ALK kinase domain were obtained at an early stage of this program; the detailed structural information from ligand–protein cocrystal structures proved to be invaluable for structure based design, particularly in addressing kinase selectivity issues (vide infra).



Two representative members **1** and **2** of a structural class of hits that emerged from an HTS screen of the Amgen compound library were intriguing. The 2-acyliminobenzimidazole kinase hinge-binding motif is not widely represented in the kinase literature.<sup>10</sup> Selected data for compounds **1** and **2** is presented in Table 1. These leads possessed significant selectivity with respect to c-Met in comparison with **3**, which is reported to have 2 nM affinity for c-Met enzyme and to have an ALK cellular potency of 20 nM.<sup>9</sup> Understanding the reason for the difference in JAK kinase selectivity between **1** and **2** was of significant interest; X-ray crystal structures of both compounds bound in the ALK kinase domain were obtained (Figure 1).<sup>11</sup> These compounds interact with the hinge region of ALK by making hydrogen bonds to Met1199 of the linker using the benzoyl carbonyl oxygen atom and a benzimidazole ring NH resulting from adoption of the exocyclic acyliminium tautomer.<sup>10</sup> The benzoyl ring sits adjacent to gatekeeper residue Leu1196. An overlay of their structures is shown in Figure 1. It appears that by very different means each molecule contrives to place a predominantly lipophilic moiety in a pocket in the enzyme defined by Leu1256, Gly1269 (the X-DFG residue at the start of the activation loop), and the backbone atoms of Arg1253/Asn1254. The sulfonamide moiety of **1** sits just below catalytic Lys1150 (but does not hydrogen bond to

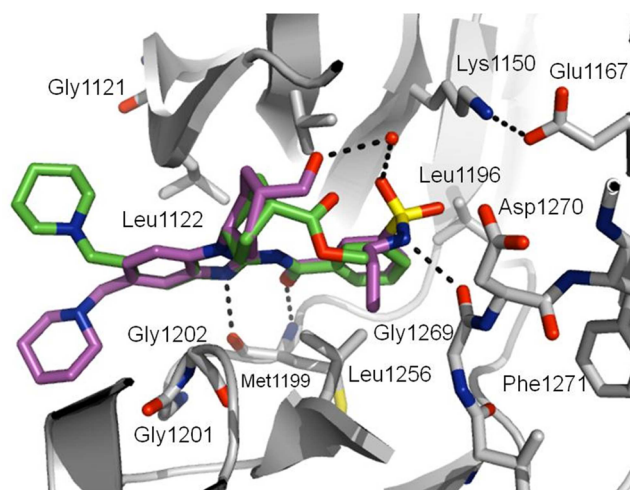


**Figure 1.** Overlay of cocrystal structures of **1** (purple) and **2** (green) in the ATP binding pocket of the ALK kinase domain. Dashed lines indicate hydrogen bonds and the red sphere denotes an ordered water molecule associated with **1**. PDB codes: **1**, 4FOB; **2**, 4FOC.

it). The sulfonamide NH forms a hydrogen bond with the backbone carbonyl of Gly1269, with the allyl appendage occupying the remainder of the lipophilic pocket; a water mediated H-bond network between the cyclohexylmethanol substituent (accommodated in the ribose binding pocket) and sulfonyl carbonyl appears to stabilize the ligand in its preferred binding conformation. Compound **2** does not engage with Gly1269, but the *cis*-1,4-disposition of the cyclohexyl carboxylate substitution pattern allows the methyl ester moiety to project into this region of the protein (which is also occupied by the fluoro-substituent of **3**<sup>11</sup>). The crystallographic data clearly indicated that a larger substituent would more effectively engage with this pocket.<sup>12</sup> Different orientations of the “water solubilizing” piperidine side chains are adopted by **1** and **2**. The piperidine moiety in **2** allowed it to reach up and apparently engage in van der Waals interactions with two backbone carbonyls on the N-terminal lobe (Gly1121, Leu1122) in a shallow pocket on the surface of the protein at the entrance to the ATP binding pocket. For compound **1**, the pendant piperidine ring points out toward residues in the C-terminal lobe (Gly1201, Glu1202, Pro 1260); its electron density was poorly defined in the crystallographic data set, indicating disorder and a lack of a distinctly preferred binding mode for this moiety.

While we did not obtain crystal structures of **1** and **2** bound to JAK2, existing JAK2 cocrystal structures permitted modeling of compounds **1** and **2** in the active site and hence development of a hypothesis for the difference in selectivity between these two potent ALK inhibitors with regard to JAK2.<sup>13</sup> As shown in Figure 2, it is notable that the ATP binding pocket of JAK2 appears to be somewhat shorter in length and narrower in width by comparison with that of ALK. Compound **2** appears

**Table 1.** Selected Data<sup>8</sup> for Screening Hit Compounds **1** and **2** in Amgen In-House Assays

no.	ALK enz IC <sub>50</sub> μM (±SD)	c-Met enz IC <sub>50</sub> μM	JAK2 enz selectivity (fold)	SRC enz selectivity (fold)	IGF1R enz selectivity (fold)	pALK cell IC <sub>50</sub> μM (±SD)	liver microsomes Cl <sub>int</sub> μL/min/mg rat/human
<b>1</b>	0.005 (±0.002)	5.92	0.4	13	60	0.048 (±0.020)	314/100
<b>2</b>	0.003 (±0.001)	ND <sup>a</sup>	64	103	15	0.054 (±0.017)	459/85

<sup>a</sup>Not determined for compound **2**; for ethyl ester analogue **14** c-Met IC<sub>50</sub> 5.12 μM.

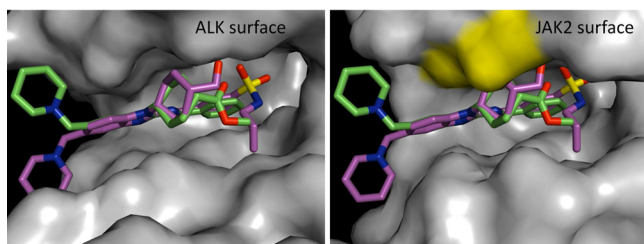


**Figure 2.** A comparison of the binding modes of compounds **1** and **2**, cocrystallized with ALK (left panel) and superimposed onto a JAK2 crystal structure (right panel). A comparison of the binding modes of compound **1** (purple) and **2** (green), cocrystallized with ALK (left panel; PBB = 4FOB and 4FOC) and superimposed onto a JAK2 crystal structure (right panel; PDB = 3LPB). The surfaces of residues Leu855 and Gly856 in JAK2 are colored yellow. Both proteins are shown at the same scale and relative orientation to illustrate differences in the dimensions of their ATP binding pockets.

unable to adopt a conformation of the cyclohexyl linkage capable of projecting the ester side chain into the corresponding affinity pocket of JAK2 due to a steric clash of the cyclohexyl linkage with residues Leu855 and Gly856 of the narrower ATP binding cavity of JAK2 (Figure 2, right panel). This may explain a significant loss in binding affinity against JAK2 vs ALK<sup>12</sup> for compound **2**. The flexible sulfonamide side chain of **1** appears able to negotiate the confines of the JAK2 protein and may reside in a very similar binding mode to that which it adopts in ALK, consistent with the similar affinity for

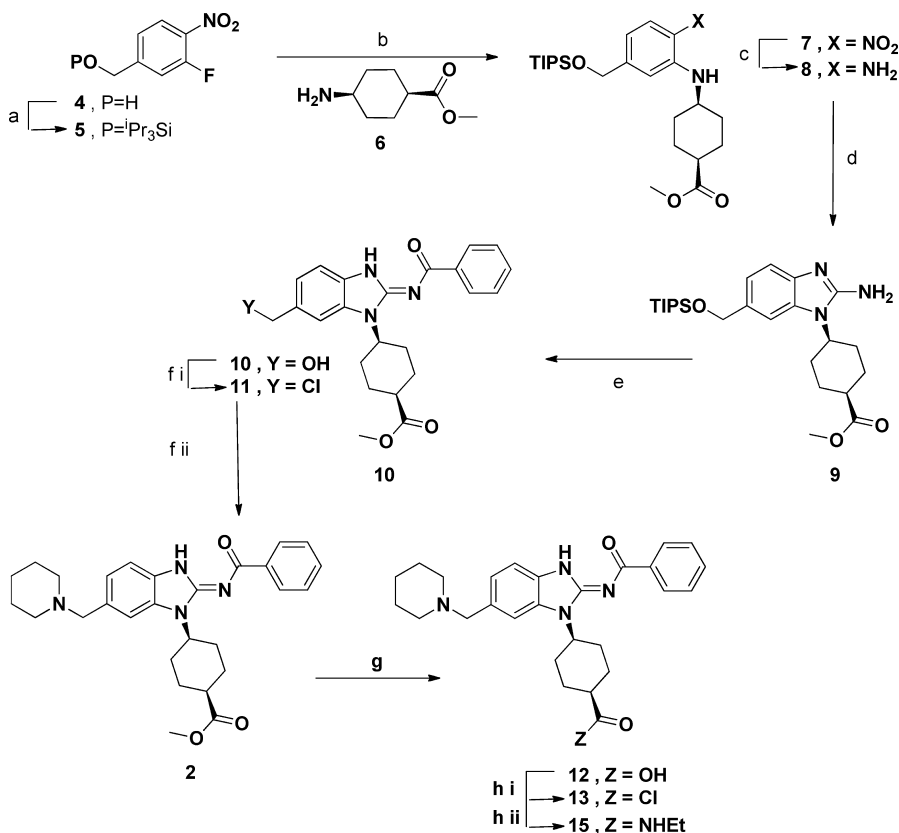
both proteins. Presumably the loss of the water bridged-hydrogen bond between the alcohol and sulfonamide functionalities is compensated by other means, allowing the cyclohexane moiety to rotate to alleviate the steric clash without incurring a major impact on the JAK2 binding energy. By virtue of the shorter cavity in JAK2 vs ALK, the surface interaction between the protein and the piperidine side chain of **2** is also potentially disrupted; it is unclear whether this contributes to the 2 orders of magnitude selectivity observed. With significant enzymatic potency, adequate cellular potency (10× enzyme-cell shift) and a working hypothesis for the understanding of the selectivity determinants based on crystallographic data, **2** represented an attractive starting point for lead optimization despite compromised in vitro microsomal stability (Table 1).

## CHEMISTRY

Compounds of this class were readily synthetically accessible.<sup>14</sup> The initial route adopted (Scheme 1) permitted independent variation of the three main structural appendages for early SAR exploration purposes.

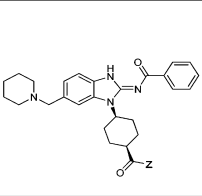
Commercially available benzyl alcohol **4** was protected as its TIPS ether, **5**, which was then subjected to  $S_NAr$  reaction with ester **6**<sup>14</sup> to afford adduct **7**. Transfer hydrogenation gave aniline **8**, which was then reacted with cyanogen bromide to give 2-aminobenzimidazole **9**. Acylation of **9** with benzoyl chloride, followed by fluoride mediated deprotection of the silyl ether, afforded benzyl alcohol **10**, which was converted into

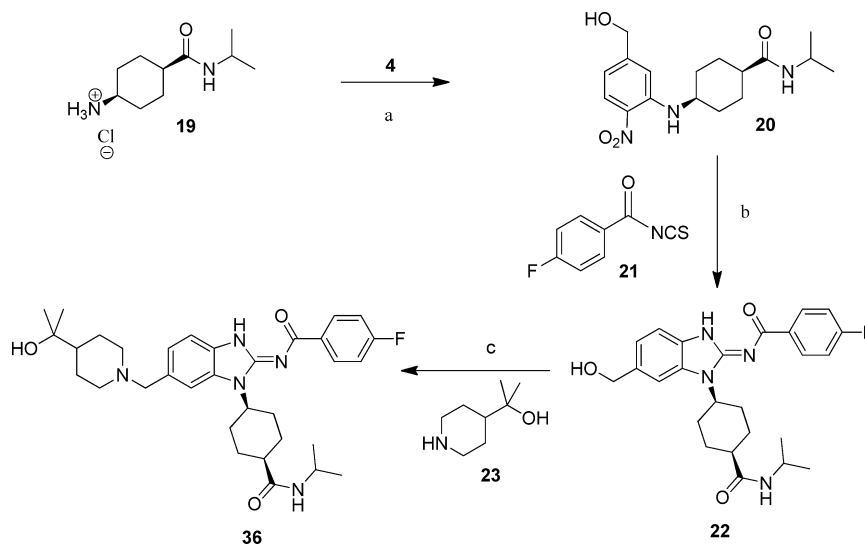
Scheme 1<sup>a</sup>



<sup>a</sup>Reagents and conditions: (a) 2,6-lutidine, TIPSOTf, DCM, 99%; (b) DIPEA, CH<sub>3</sub>CN, 50 °C, 60%; (c) NH<sub>4</sub>HCO<sub>2</sub>, 10% Pd/C, EtOH, 100%; (d) CNBr, EtOH, 25 °C, 92%; (e) (i) PhCOCl, Et<sub>3</sub>N, DCM, 0 °C, (ii) TBAF, THF, 0–25 °C, 63%; (f) (i) SOCl<sub>2</sub>, 0 °C, (ii) piperidine, DMSO, 25 °C, 75%; (g) NaOH, MeOH, 95%; (h) (i) SOCl<sub>2</sub>, neat, 0 °C, (ii) EtNH<sub>2</sub>, THF 0–25 °C, 90%.

Table 2. Cyclohexylcarboxyl SAR<sup>8</sup> Affords a Means of Achieving Selectivity over JAK2

#		ALK enz IC <sub>50</sub> μM	JAK2 Selectivity (fold)	SRC Selectivity (fold)	IGF1R Selectivity (fold)	pALK cell IC <sub>50</sub> μM	Liver microsomes Ch <sub>int</sub> μl/min/mg
							Rat / Human
2	OMe	0.003	64	103	15	0.054	459 / 85
14	OEt	0.001	244	61	18	0.018	706 / 222
15	NHEt	0.002	781	246	29	0.007	310 / 194
16	N(Et) <sub>2</sub>	0.024	91	121	24	0.562	682 / 364
17	NH <sub>2</sub>	0.018	463	86	2	0.044	129 / 61
18	NH <sup>t</sup> Pr	0.002	813	429	36	0.005	389 / 203

Scheme 2<sup>a</sup>

<sup>a</sup>Reagents and conditions: (a) <sup>t</sup>Pr<sub>2</sub>EtN, CH<sub>3</sub>CN, 50 °C, 71%; (b) (i) H<sub>2</sub>/10% Pd/C, EtOH, (ii) **21**, THF, (iii) EDCI, <sup>t</sup>Pr<sub>2</sub>EtN, 80% overall; (c) (i) SOCl<sub>2</sub>, 0 °C, (ii) **23**, DCM, 25 °C; 56% overall.

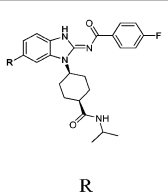
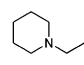
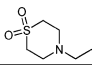
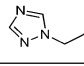
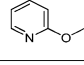
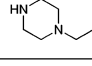
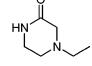
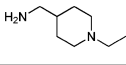
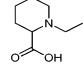
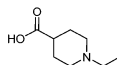
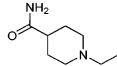
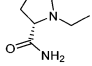
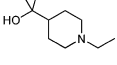
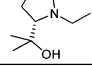
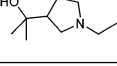
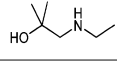
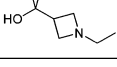
benzyl chloride **11** using thionyl chloride and then displaced with piperidine to give **2**. Saponification of the methyl ester, conversion of the resulting acid **12** to acid chloride **13**, and subsequent treatment with ethylamine gave compound **15**. The substitution of ethylamine with other nucleophiles gave access to the compounds shown in Table 2.

For optimization of the piperidine moiety, the order of steps in the synthetic route was modified to allow more efficient access to SAR in this region of the molecule: the invariant isopropyl carboxamide would be installed early in the sequence (Scheme 2). Thus isopropyl amide **19**<sup>14</sup> underwent S<sub>N</sub>Ar reaction with 3-fluoro-4-nitrobenzyl alcohol **4** to give adduct

**20**, which was reduced to the diamine and then reacted with 4-fluorobenzoyl isothiocyanate **21**. Benzimidazole ring closure was effected in situ by treatment with EDCI to afford **22**. Finally, the benzyl alcohol of **22** was converted to the corresponding benzyl chloride on exposure to thionyl chloride and then reacted with with **23** to produce **36**. Substitution of piperidine **23** with the nucleophile of choice gave the compounds in Table 3.

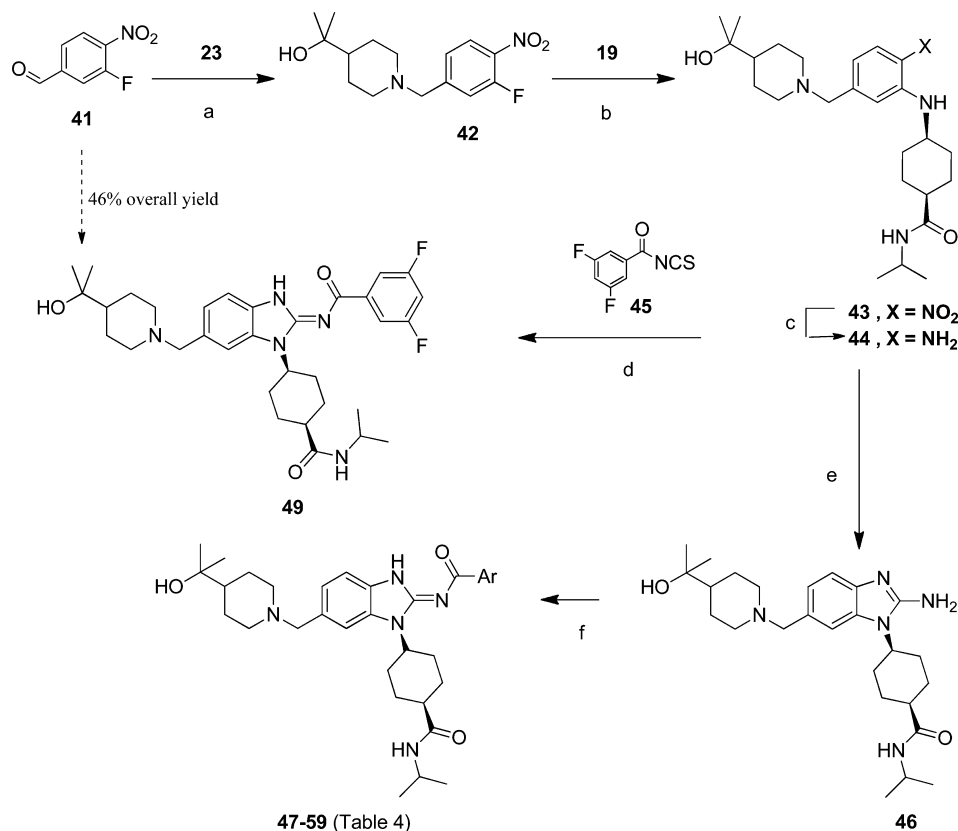
A further modification to the route was made to explore a diversity of benzoyl substituents (Scheme 3). Reductive amination of benzaldehyde **41** with amine **23** gave adduct **42**, which underwent S<sub>N</sub>Ar with amine **19** and was then reduced to

Table 3. Selected Piperidine Replacement SAR<sup>8</sup> Addressing Metabolic Stability

#		ALK enz IC <sub>50</sub> μM (±SD)	JAK2 Selectivity (fold)	SRC Selectivity (fold)	IGF1R Selectivity (fold)	pALK cell IC <sub>50</sub> μM (±SD)	Liver microsomes Cl <sub>int</sub> μL/min/mg	Rat (IV)Clp L/Kg/h
							Rat / Human	
24	H	0.007	410	118	72	0.147	392 / 345	ND
25		0.0016 (±0.0001)	356	84	28	0.004 (±0.002)	451 / 302	ND
26		0.002 (±0.001)	115	125	53	0.008 (±0.004)	304 / 380	4.08
27		0.002	300	93	48	0.004	286 / 436	8.19
28		0.0083 (±0.0004)	240	155	50	0.109 (±0.027)	127 / 152	2.25
29		0.0016 (±0.0001)	530	104	39	0.005 (±0.001)	43 / 42	5.78
30		0.002	270	94	44	0.006	45 / 194	10.8
31		0.0012 (±0.0001)	776	223	46	0.008 (±0.002)	<14 / 26	0.92
32		0.003	154	61	31	0.144	<14 / <14	ND
33		0.002	450	99	50	0.345	<14 / <14	ND
34		0.0014 (±0.0003)	350	152	54	0.004 (±0.002)	45 / 9	6.44
35		0.002	488	211	38	0.008	1178 / 1212	ND
36		0.0012 (±0.0002)	641	148	61	0.004 (±0.002)	15 / 51	0.81
37		0.0026 (±0.0003)	298	134	37	0.013 (±0.008)	455 / 569	ND
38		0.0019 (±0.0003)	427	106	33	0.008 (±0.004)	57 / 181	1.41
39		0.001	915	165	61	0.0016 (±0.0000)	68 / 233	1.3
40		0.0015 (±0.0001)	640	194	62	0.002 (±0.001)	<14 / 105	0.89

diamine **44**. For exploration of benzamide SAR, **44** was reacted with acetyl isothiocyanate, ring closure was effected with EDCI, and the acetyl protecting group cleaved by acidic hydrolysis to afford aminobenzimidazole **46** as a key precursor for

subsequent benzoylation. EDCI/HOBt coupling conditions were not particularly efficient on this substrate (yields of 15–24% were typical), however, the procedure was widely applicable. Ultimately, this route was adapted for an efficient

Scheme 3<sup>a</sup>

<sup>a</sup>Reagents and conditions: (a) Na(AcO)<sub>3</sub>BH, DCM, 88%; (b) <sup>i</sup>Pr<sub>2</sub>EtN, CH<sub>3</sub>CN, 50 °C, 73%; (c) NH<sub>4</sub>HCO<sub>2</sub>, Pd/C, EtOH, 100%; (d) <sup>i</sup>Pr<sub>2</sub>EtN/EDCI, 72%; (e) (i) MeCONCS, dioxan, 100 °C, (ii) EDCI, <sup>i</sup>Pr<sub>2</sub>EtN, 60 °C, HCl aq (2N), 50 °C, 82% overall; (f) ArCO<sub>2</sub>H, EDCI, HOBT, <sup>i</sup>Pr<sub>2</sub>EtN, DMF, 50 °C, 15–24%

larger scale synthesis of compounds advancing to animal studies. The diamine **44** reacted smoothly with benzoyl isothiocyanates such as **45** (conveniently generated by the action of potassium isothiocyanate on the corresponding benzoyl chloride), followed by EDCI mediated ring closure to give good yields (72% for **49**) of final product (46% overall from benzaldehyde **41**).

## RESULTS AND DISCUSSION

Ester **2** afforded a good starting point in terms of potent enzymatic inhibition of ALK. However, significant improvements to cellular potency, off-target kinase selectivity profile, and a dramatic improvement in metabolic stability were required. A brief examination of SAR of the methyl ester moiety of **2** (Table 2) indicated that replacement of the ester moiety of **14** with an ethyl amide **15** afforded an improvement in cellular potency, together with significant enhancement of selectivity against JAK2. A modest impact on SRC selectivity was noted, without significant change in selectivity against IGF1R.

An unsubstituted primary amide **17**, or bis-substitution of the amide nitrogen **16**, resulted in a significant loss in both cellular and enzymatic potency and consequent erosion in selectivity against SRC. From a wide range of ester and amide isosteres and alternative alkyl substituents explored (data not shown), the isopropyl amide **18** emerged as offering the most atom efficient combination of cellular potency and selectivity. It was also noted that the primary amide **17** displayed significantly improved microsomal stability<sup>16</sup> in comparison with the more

elaborate derivatives. Oxidative N-dealkylation of the amide was observed to be a significant metabolic pathway in liver microsomal incubations. A second site of extensive metabolism was, as expected, the piperidine moiety. A wide variety of changes to this part of the molecule were explored, and a selection of the more informative is included in Table 3. A variety of standard techniques to modify the basicity of the nitrogen (e.g., **26**) retained the cell potency but also retained the poor microsomal stability of lead **25**. Attempts to block metabolism by the introduction of steric crowding in the vicinity of the amine nitrogen led to a loss of potency. Complete excision of the side chain (**24**) resulted in a 35-fold loss in cellular potency without impacting microsomal stability. A range of aromatic heterocyclic replacements for the piperidine were explored, again without utility. Typically these compounds either retained cellular potency but had marginal impact on microsomal stability as with triazole (**27**) or suffered from a significant loss in cellular potency as with pyridine **28**. Interestingly, piperazine **29** retained cellular potency and displayed a marked improvement in microsomal stability but had clearance greater than liver blood flow on IV dosing in rat. Piperidinone analogue **30** behaved likewise, however, 4-aminomethylpiperidine **31** displayed astonishing microsomal stability, which translated into improved rat IV clearance amounting to 30% of liver blood flow. As a result of this unexpected finding, a wide range of polar substituents were explored in a variety of configurations. Carboxylic acids such as **32** and **33** furnished zwitterions which were stable toward microsomal transformation, however, cellular potency was

significantly impacted. The primary amides of these acids were investigated and found to retain cellular potency, however, they varied significantly in their microsomal stability depending on the location of the amide moiety; compare, for example, **34** and **35**. The most promising, **34**, was found to have high clearance on IV dosing in rat. A tertiary alcohol at the 4-position of the piperidine ring **36** recapitulated the remarkable metabolic stability of amine **31** and displayed good PK properties in rat (vide infra). The disposition of the alcohol substituent relative to the amine was important for controlling the in vitro metabolic stability of this class of molecule. Analogues **36** and **40** shared the improved PK characteristics of **31**, whereas analogues **37**, **38** and **39** were less optimal. Tertiary alcohol **36** appeared to be optimal. These observations lead us to speculate that a correctly placed polar moiety influences microsomal stability by perturbing CYP molecular recognition; docking of the molecule in the active site of the metabolizing CYP<sub>450</sub> in an orientation that presents the metabolic soft spots to the catalytic heme is disfavored.

X-ray crystallography (Figure 3) shows that the benzamide motif of **36** sits deep in the ATP binding site of the kinase, in

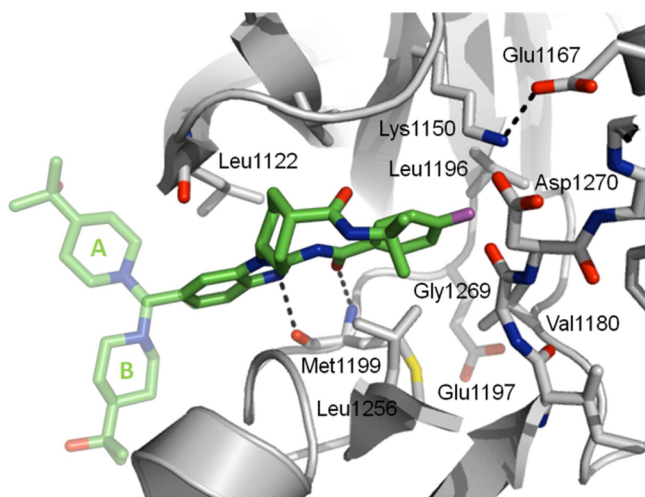


**Figure 3.** Co-crystal structure of ALK with compound **36**. The solubilizing group is observed to adopt two possible orientations (A or B). Dashed lines indicate hydrogen bonds. PDB code is 4FOD.

relatively close proximity to gatekeeper residue, Leu 1196, in a pocket also defined by Val1180 and Leu1256. It was therefore anticipated that the substitution pattern of the aryl ring may permit fine-tuning of the kinase selectivity profile.<sup>15</sup> In exploration of the SAR of the iminobenzamide moiety, it was necessary to retain the bias toward the exocyclic acylimine tautomer in order to maintain key H-bond donor–acceptor interactions with the hinge region of the kinase. This tautomer is favored by extended  $\pi$ -delocalization into the pendant aryl ring, achieved by retaining a coplanar arrangement between benzamide and benzimidazole moieties.<sup>10</sup> The SAR was necessarily constrained to aryl or heteroaryl substituents lacking ortho-substitution to avoid steric or lone-pair–lone-pair peri-interactions, disrupting the optimal coplanar disposition of these moieties. In the crystal structure of **36**, there is also evidence of a favorable interaction between the ortho-CH and backbone carbonyl of Glu1197 (3.2 Å), which was desirable to preserve. Initial SAR studies (Table 4) concentrated on the evaluation and optimization of selectivity over the related SRC

and IGF1R kinases, with an expectation that the cyclohexylbenzamide motif would provide the necessary selectivity over the JAK family kinases as discussed above. Overall, this proved to be correct, however, it was notable that meta- or para- cyano substituents (**55**, **51**) resulted in a measurable erosion of selectivity against JAK 2. Table 4 illustrates a selection of substitution patterns that retained high enzymatic potency on ALK. *meta*-Chloro or -cyano substituents (**54**, **55**, **57**, **58**) conferred improved IGF1R selectivity as did *meta*-pyridyl **52**, however, these changes resulted in compromised cellular activity against ALK. The cellular context was used to drive SAR development, as this strategy provided a means of identifying those compounds most likely to have superior potency in vivo. Fluoro substituents were well tolerated at the meta- and para- positions (**36**, **48**, **49**, **53**) and retained the low ALK enzyme cell shift of the parent benzamide.

Analogues with acceptable selectivity profiles (>50-fold) and liver microsomal stability indicative of modest clearance were progressed to rat PK, where *p*-fluoro analogue **36** and 3,5-difluoro analogue **49** had acceptable PK distribution and clearance parameters and were therefore progressed to beagle dog PK, where results were superior to the rat (Table 5). Plasma protein binding in dog was comparable with that measured in human plasma. The bioavailability obtained with an unoptimized formulation was considered acceptable at this stage and prompted further profiling of these two molecules. Routes of metabolism studies for both **36** and **49** in isolated liver microsomes indicated that the principal oxidated transformations were oxidative hydrolysis of the piperidine ring, leading to a primary benzylamine as an observable metabolite as well as oxidative dealkylation of the isopropyl amide moiety to afford a primary cyclohexylcarboxamide. These metabolites were observed in the microsomal incubations of all four species studied (mouse, rat, dog, human). Oxidations on the core molecular scaffold were not observed.

Both compounds were profiled against an Ambit panel of 442 kinases, which indicated that the difluoroaryl ring of **49** conferred an overall superior selectivity profile in comparison with **36** as indicated by the kinome tree plots of Figure 4. The S(10) selectivity score was 0.07 for **36** and 0.036 for **49**. Selected kinases identified from the most active hits in the Ambit kinome panel were followed up with titrated  $K_d$  determinations, shown in Table 6.

Insulin receptor (INSR) activity was followed up separately in a functional cellular context;<sup>18</sup> pINSR activity was measured for both compounds: **49** pINSR IC<sub>50</sub> 536 nM (pALK IC<sub>50</sub> 5.5 nM; 97-fold selective) and **36** pINSR IC<sub>50</sub> 231 nM (pALK IC<sub>50</sub> 6.0 nM; 38-fold selective).

Compounds **36** and **49** were also profiled against ALK enzymes bearing point mutations R1275Q or L1196M and were found to fully retain their potency against these mutants.<sup>19</sup> The L1196 M “gatekeeper mutation” has been observed clinically in patients with developed resistance to crizotinib.<sup>5</sup>

Upon examination of compound **36** in a murine PD model,<sup>20</sup> very rapid clearance of the compound from plasma was observed; the clearance mechanism was traced to a murine-specific amidase, resulting in cleavage of the benzamide moiety. The compound was not subject to this route of metabolism in rat, dog, or human whole blood, but it did limit the value of performing further experiments in mice with **36**. A detailed study of the mechanism, kinetics, and SAR of this mode of metabolism will be reported elsewhere.<sup>21</sup> In contrast, close analogue **49** had significantly better mouse PK ( $T_{1/2}$  (IV) 1.05

Table 4. Optimization of the Acylbenzamide Moiety to Enhance Kinase Selectivity<sup>8</sup>

#		pALK cell IC <sub>50</sub> μM (±SD)	ALK enz IC <sub>50</sub> μM (±SD)	JAK2 fold selectivity	SRC fold selectivity	IGF1R fold selectivity	Rat/ Human Liver microsomes Cl <sub>int</sub> ul/min/mg
47		0.004 (±0.003)	0.002	597	418	48	21/ 40
36		0.004 (±0.002)	0.001 (±0.0002)	641	148	61	15/ 51
48		0.003 (±0.002)	0.001 (±0.0001)	959	570	100	10/ 102
49		0.006 (±0.001)	0.001 (±0.0002)	1072	427	107	48/ 87
50		0.008 (±0.008)	0.001	719	47	33	<14/ 57
51		0.002 (±0.001)	0.001	174	21	63	31/ 106
52		0.035	0.006	260	40	54	<14/ 47
53		0.007	0.002	301	53	37	19/ 60
54		0.048	0.003	268	112	278	30/ 90
55		0.015	0.001	278	206	411	17/ 72
56		0.333	0.003	799	402	466	43/ 83
57		0.072	0.002	750	355	173	24/ 78
58		0.074	0.003	480	47	165	44/ 83
59		0.004	0.001	318	26	131	29/ 132

h), which permitted evaluation in a range of pharmacodynamic (PD) and tumor xenograft models of ALK driven disease.<sup>20</sup> In particular, compound **49** exhibited dose-dependent inhibition in an NPM-ALK driven tumor xenograft model utilizing the

Karpas-299 cell line, Figure 5. Approximately 10–12 days after Karpas-299 cell implantation, SCID-beige mice with well-formed tumors of similar size were placed into groups ( $n = 10/\text{group}$ ) so that the average tumor size was similar in each group



Table 5. Pharmacokinetic Parameters and Plasma Protein Binding Measured for Compounds 36 and 49

no.	rat				dog				plasma protein binding %		
	V <sub>ss</sub> L/kg	Cl <sub>p</sub> L/kg/h	T <sub>1/2</sub> (IV) h	F %	V <sub>ss</sub> L/kg	Cl <sub>p</sub> L/kg/h	T <sub>1/2</sub> (IV) h	F %	rat	dog	human
36	6.4	0.813	5.6	20	1.58	0.201	5.7	52	92.5	94.8	94.7
49	5.42	0.717	5.8	11	1.82	0.167	7.9	71	95.1	97.8	96.3

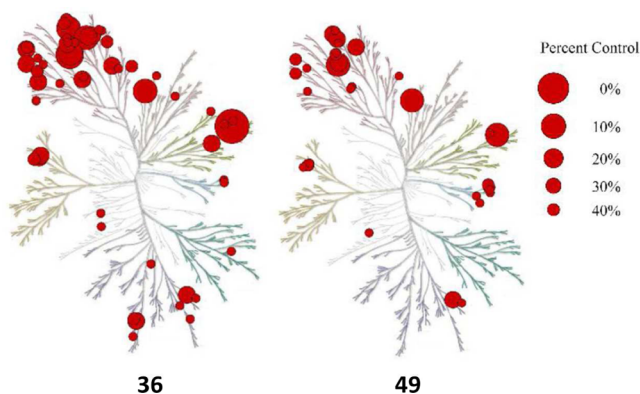


Figure 4. AMBIT kinome screening at 1  $\mu\text{M}$ , annotated on ( $n = 442$ ) enzymes in the human 36 and 49 with hits showing % control at 1  $\mu\text{M}$  (i.e., 0%, largest spot is most active) overlaid on the kinome phylogenetic tree.<sup>17</sup>

Table 6. Selected Ambit Kinome Panel Data (442 Kinases from the Human Kinome with POC Data Generated at 1.0  $\mu\text{M}$  Compound Concentration) with Titrated  $K_d$  Follow Up

kinase	36			49		
	POC at 1 $\mu\text{M}$	Ambit titrated $K_d$ (nM)	selectivity vs ALK	POC at 1 $\mu\text{M}$	Ambit titrated $K_d$ (nM)	selectivity vs ALK
ALK	0.55	0.36	1	2.7	0.24	1
AXL	0.75	29	80	82	1600	6656
FLT3	7.9	42	116	42	ND	ND
INSR	16	ND	ND	38	72	300
IRAK1	0.2	5.7	16	0.15	5.6	23
LCK	1	28	77	6.4	110	458
LTK	0.1	2.5	7	0.35	8.2	34
MAP4K2	0.05	11	31	0.35	25	104
MER	1.3	18	50	1	72	300

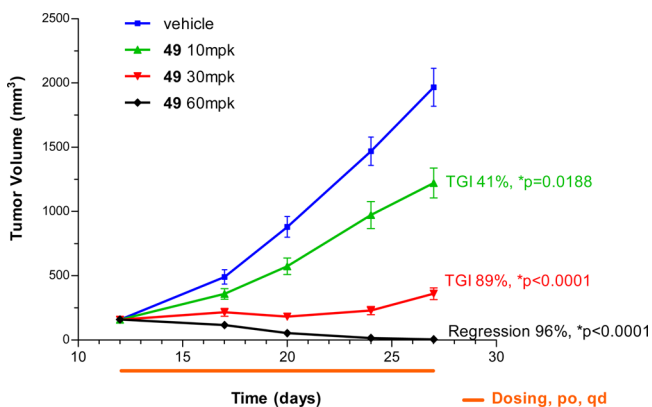


Figure 5. Compound 49 dosed (10, 30, 60 mpk, po, qd) in SCID-beige mice bearing Karpas-299 xenografts. \*\*After 15 days of treatment with 49 at the 60 mpk dose, the tumors in 6 of the 10 animals had completely regressed. See Supporting Information Figure S1 for body weight data from this study.

(ranging from approximately 150–250  $\text{mm}^3$ ) at initiation of dosing. Compound was dosed orally (po) at 10, 30, or 60 mg/kilogram (mpk), once daily (qd); tumor volume was assessed for each animal periodically over the 15 day treatment period and compared with tumors growing in a vehicle control group; \* $p$  values were calculated using RMANOVA with Dunnett's comparison. A 10 mpk qd dose of 49 resulted in observed tumor growth inhibition (TGI) of 41% (\* $p = 0.019$ ) after 15 days of dosing. At 30 mpk qd 89% (\* $p < 0.0001$ ) TGI was observed at day 15. Furthermore, a 60 mpk qd dose of 49 over the same period led to 96% (\* $p < 0.0001$ ) tumor regression, with no visible tumor remaining in 6 of 10 animals at study termination. The compound was very well tolerated by the animals at all tested doses, as assessed by minimal change in body weight observed over the course of the study.<sup>20</sup>

Terminal PK measurement following the final dose indicated that the 60 mpk dose maintained a plasma free fraction level of drug above the cellular  $\text{IC}_{50}$  for 17 h post dose, with target  $\text{IC}_{50}$  coverage exceeding 13 h at the 30 mpk dose. The data provides an indication of the benefits of extended duration of target coverage over the cellular  $\text{IC}_{50}$ , resulting in substantial tumor regression in this model.

## CONCLUSION

A class of 2-acyliminobenzimidazoles was identified as potent and selective inhibitors of anaplastic lymphoma kinase. Structure based design was instrumental in developing an understanding of SAR and facilitated the optimization of kinase selectivity. Introduction of an optimally placed polar substituent was key to solving issues of metabolic stability and led to the development of potent orally bioavailable ALK inhibitors with substantial in vivo potency in an ALK-driven xenograft model of cancer. These compounds appear to be able to better retain their potency against point mutations in the enzyme which are thought to confer resistance to crizotinib. Compounds from this class have significant promise for development as useful therapeutics for the treatment of ALK driven cancers.<sup>22</sup> Additional in vivo characterization of these molecules will be the subject of subsequent publications.

## EXPERIMENTAL DETAILS

**General.** All reagents and solvents were obtained from commercial suppliers and used without further purification. Silica gel chromatography was performed using prepacked silica gel cartridges (ISCO).  $^1\text{H}$  NMR spectra were obtained on either a Bruker Avance 1 400 MHz spectrometer or a Bruker Avance 2 600 MHz spectrometer with a 5 mm TXI cryoprobe using the residual solvent peak as the reference. All tested compounds were purified to >95% purity at 215 and 254 nm as determined by HPLC. HPLC analysis was obtained on an Agilent 1100 system, using an Agilent Zorbax SB-C8 column (150 mm  $\times$  4.6 mm, 5  $\mu$ ) at 40  $^\circ\text{C}$  with a 1.5 mL/min flow rate using a gradient of 5–100% [0.1% TFA in acetonitrile] in [0.1% TFA in water] over 15 min. Electrospray mass (ESI) measurements were obtained on an Agilent 1100 series LC/MSD system, using one of the following two separation methods: [A] Agilent Zorbax SB-C18 column (50 mm  $\times$  3.0 mm, 3.5  $\mu$ ) at 40  $^\circ\text{C}$  and a gradient of 5–95% [0.1% TFA in acetonitrile] in [0.1% TFA in water] over 3.5 min; [B] Phenomenex

Gemini C18 column (50 mm × 3.0 mm, 3 μ) at 40 °C with a 1.5 mL/min flow rate using a gradient of 5–95% [0.1% formic acid in acetonitrile] in [0.1% formic acid in water] over 3.5 min. Preparative HPLC was performed on one of two systems: (A) Gilson preparative HPLC system using a Phenomenex Gemini-NX C18 110A column (100 mm × 21 mm, 5 μ); (B) Agilent mass-directed preparative HPLC system using an xBridge C18 column (100 mm × 19 mm, 10 μ). Exact mass (HRMS) measurements were performed on an Agilent 1100 HPLC by flow injection analysis, eluting with [1:1 water/ acetonitrile with 0.1% formic acid] at 2 mL/min, with MS detection by an Agilent G1969A time-of-flight (TOF) mass spectrometer.

**(3-Fluoro-4-nitrobenzyl)oxytriisopropylsilane (5).** To a solution of **4** (Bionet, 4.7 g, 27.5 mmol) in DCM (47 mL) was added triisopropylsilyl trifluoromethanesulfonate (9.26 g, 30.2 mmol) and 2,6-dimethylpyridine (3.53 g, 33.0 mmol). The resulting mixture was stirred for 3 h at ambient temperature and then washed with saturated aqueous ammonium chloride and water. The organic layer was collected, dried over sodium sulfate, filtered, and concentrated to produce **5** (8.9 g, 99% yield) as a light-yellow oil.

**(1s,4s)-Methyl 4-Aminocyclohexanecarboxylate (6).** To a solution of (1s,4s)-4-aminocyclohexanecarboxylic acid (15 g, 105 mmol) in methanol (150 mL) was added sulfuric acid (10.27 g, 105 mmol), and the reaction was stirred at 80 °C for 18 h. The reaction mixture was then cooled to 0 °C, neutralized with aqueous ammonium hydroxide, and extracted with DCM. The organic layer was dried over sodium sulfate, filtered, and concentrated to afford **6** (16.00 g, 97% yield) as a light-yellow oil. <sup>1</sup>H NMR (400 MHz, CDCl<sub>3</sub>) δ 3.68 (s, 3 H), 2.86–2.92 (m, 1 H), 2.34–2.58 (m, 1 H), 2.14 (br s, 2 H), 2.00–2.06 (m, 2 H), 1.66–1.78 (m, 2 H), 1.54–1.66 (m, 2 H), 1.32–1.50 (m, 2 H).

**(1s,4s)-Methyl 4-((2-Nitro-5-(((triisopropylsilyloxy)methyl)phenyl)amino)cyclohexanecarboxylate (7).** To a solution of **5** (6.3 g, 19.2) and **6** (3.63 g, 23.1 mmol) in acetonitrile (32 mL) was added *N,N*-diisopropylethylamine (10.0 mL, 57.7 mmol), and the reaction mixture was stirred at 50 °C for 20 h. After the reaction was complete, the reaction mixture was allowed to cool to ambient temperature and diluted with water (20 mL) and DCM (50 mL). The organic layer was collected, dried over anhydrous sodium sulfate, filtered, and concentrated. The crude product was purified by column chromatography, eluting with 10–30% ethyl acetate in hexanes, to produce **7** (5.35 g, 60% yield) as an orange solid.

**(1s,4s)-Methyl 4-(2-Amino-5-(((triisopropylsilyloxy)methyl)phenyl)amino)cyclohexanecarboxylate (8).** To a solution of **7** (2.80 g, 6.0 mmol) in ethanol (48.5 mL), under a nitrogen atmosphere, was added 10% palladium on carbon (0.65 g, 0.6 mmol) and ammonium formate (3.79 g, 60.0 mmol). The reaction was stirred at ambient temperature for 2 h and then filtered through a Celite pad. The filter cake was rinsed with ethanol and DCM, and the combined filtrates were concentrated and partitioned between DCM and water. The organic portion was dried over anhydrous sodium sulfate, filtered, and concentrated to afford **8** (2.61 g, 100% yield) as a purple oil. LC/MS (ESI<sup>+</sup>) *m/z* = 435.2 (M + H).

**(1s,4s)-Methyl 4-(2-Amino-6-(((triisopropylsilyloxy)methyl)-1H-benzo[d]imidazol-1-yl)cyclohexanecarboxylate (9).** To a solution of **8** (2.50 g, 5.8 mmol) in ethanol was added cyanogen bromide (0.91 g, 8.6 mmol), and the reaction was stirred at ambient temperature for 16 h. The reaction mixture was concentrated in vacuo, diluted with DCM, and washed with aqueous sodium hydroxide. The organic portion was dried over anhydrous sodium sulfate, filtered, and concentrated to afford **9** (2.4 g, 92% yield) as a brown solid. LC/MS (ESI<sup>+</sup>) *m/z* = 460.2 (M + H).

**(1s,4s)-Methyl 4-((E)-2-(Benzoylimino)-6-(hydroxymethyl)-2,3-dihydro-1H-benzo[d]imidazol-1-yl)-cyclohexanecarboxylate (10).** Step 1: To a solution of benzoyl chloride (0.33 g, 2.3 mmol) in dichloromethane (7.3 mL), cooled to 0 °C, was added **9** (1.00 g, 2.2 mmol) portionwise, followed by triethylamine (1.21 mL, 8.7 mmol). The reaction was stirred at 0 °C for 30 min. The ice bath was then removed, and the reaction was stirred at ambient temperature for 1 h. The reaction mixture was partitioned between aqueous ammonium chloride and DCM. The

organic portion was dried over sodium sulfate, filtered, and concentrated to afford (1s,4s)-methyl 4-((E)-2-(benzoylimino)-6-(((triisopropylsilyloxy)methyl)-2,3-dihydro-1H-benzo[d]imidazol-1-yl)cyclohexanecarboxylate as a brown oil.

Step 2: To a solution of (1s,4s)-methyl 4-((E)-2-(benzoylimino)-6-(((triisopropylsilyloxy)methyl)-2,3-dihydro-1H-benzo[d]imidazol-1-yl)cyclohexanecarboxylate (1.22 g, 2.2 mmol) in THF (4.33 mL), cooled to 0 °C, was added a 1 M solution of tetrabutylammonium fluoride in THF (3.30 mL, 3.3 mmol) dropwise. The reaction was stirred at 0 °C for 15 min and then stirred at ambient temperature for 2 h. The reaction mixture was quenched with water and diluted with DCM. The organic portion was dried over sodium sulfate, filtered, and concentrated. The crude product was purified by column chromatography, eluting with 30–50% ethyl acetate in hexanes, to afford **10** (0.56 g, 63% yield). LC/MS (ESI<sup>+</sup>) *m/z* = 408.2 (M + H).

**(1s,4s)-Methyl 4-((E)-2-(Benzoylimino)-6-(chloromethyl)-2,3-dihydro-1H-benzo[d]imidazol-1-yl)cyclohexanecarboxylate (11).** To a solution of **10** (0.40 g, 0.98 mmol) in DCM (9.8 mL), cooled to 0 °C, was added thionyl chloride (1.43 mL, 19.6 mmol) dropwise. The reaction was stirred at 0 °C for 15 min and then stirred at ambient temperature for 30 min. The reaction mixture was then concentrated in vacuo to afford **11** as a white solid. LC/MS (ESI<sup>+</sup>) *m/z* = 426.2 (M + H).

**(1s,4s)-Methyl 4-((E)-2-(Benzoylimino)-6-(piperidin-1-ylmethyl)-2,3-dihydro-1H-benzo[d]imidazol-1-yl)-cyclohexanecarboxylate (2).** To a solution of **11** (0.41 g, 0.96 mmol) in DMSO (4 mL) was added piperidine (0.97 mL, 9.8 mmol) dropwise. The reaction was stirred at ambient temperature for 1 h. The reaction mixture was then diluted with DCM and washed with water. The organic layer was dried over sodium sulfate, filtered, and concentrated. The residue was triturated with 10% water in methanol to afford **2** (0.34 g, 75% yield) as a white solid. <sup>1</sup>H NMR (400 MHz, DMSO-*d*<sub>6</sub>) δ 12.80 (br s, 1 H), 8.11–8.21 (m, 2 H), 7.36–7.58 (m, 5 H), 7.13 (d, *J* = 8.03 Hz, 1 H), 4.62–4.88 (m, 1 H), 3.77 (s, 3H), 3.50 (br s, 2 H), 2.80–2.91 (m, 1 H), 2.53–2.71 (m, 2 H), 2.19–2.43 (m, 6 H), 1.62–1.93 (m, 4 H), 1.35–1.60 (m, 6 H). HRMS (*m/z*): [MH<sup>+</sup>] calcd for C<sub>28</sub>H<sub>33</sub>N<sub>4</sub>O<sub>3</sub>, 475.2704; found, 475.2705.

**(1s,4s)-Ethyl 4-((E)-2-(Benzoylimino)-6-(piperidin-1-ylmethyl)-2,3-dihydro-1H-benzo[d]imidazol-1-yl)-cyclohexanecarboxylate (14).** Compound **14** was prepared according to the reaction sequence described for the synthesis of **2**, substituting ethanol for methanol in the first step to afford the ethyl ester. <sup>1</sup>H NMR (400 MHz, CDCl<sub>3</sub>) δ 8.31–8.35 (m, 2 H), 7.35–7.68 (m, 6 H), 4.28 (q, *J* = 7.11 Hz, 2 H), 4.23–4.26 (m, 1 H), 3.38–3.55 (m, 2 H), 2.47–2.89 (m, 5 H), 2.24–2.44 (m, 4 H), 1.80–1.98 (m, 8 H), 1.58–1.70 (m, 2 H), 1.34 (t, *J* = 7.09 Hz, 3 H). HRMS (*m/z*): [MH<sup>+</sup>] calcd for C<sub>29</sub>H<sub>37</sub>N<sub>4</sub>O<sub>3</sub>, 489.2860; found, 489.2867.

**Preparation of 15–18. General Procedure A.** Step 1: To a suspension of **2** (0.23 g, 0.49 mmol) in methanol (7 mL) was added 1 N aqueous sodium hydroxide (7.3 mL, 7.3 mmol), and the resulting mixture was stirred at ambient temperature overnight. The reaction was neutralized with 1 N aqueous HCl and extracted with DCM (50 mL). The organic portion was dried over sodium sulfate, filtered, and concentrated to afford **12**.

Step 2: A suspension of **12** (50 mg, 0.11 mmol) in thionyl chloride (0.5 mL) was stirred at ambient temperature for 30 min. The reaction mixture was then concentrated in vacuo, and the residue was suspended in THF (1.1 mL), cooled to 0 °C, and treated with an amine (0.11 mmol). The resulting mixture was stirred at 0 °C for 30 min and then stirred at ambient temperature for 1 h. The reaction mixture was partitioned between water and DCM. The organic portion was dried over anhydrous sodium sulfate, filtered, and concentrated to afford the desired product.

**(E)-N-(1-((1s,4s)-4-(Ethylcarbamoyl)cyclohexyl)-6-(piperidin-1-ylmethyl)-1H-benzo[d]imidazol-2(3H)-ylidene)benzamide (15).** General procedure A, with ethylamine, was used to produce **15** (40 mg, 76% yield). <sup>1</sup>H NMR (400 MHz, DMSO-*d*<sub>6</sub>) δ 9.98 (br s, 1 H), 8.23–8.31 (m, 2 H), 7.90 (s, 1 H), 7.83–7.88 (m, 1 H), 7.60 (d, *J* = 8.02 Hz, 1 H), 7.37–7.57 (m, 4 H), 4.58–4.83 (m, 1 H), 4.33 (m, 2 H), 3.38 (m, 2 H), 3.16–3.28 (m, 2 H), 2.69–2.97 (m, 4 H), 2.18 (m, 2 H), 1.59–1.88 (m, 9 H), 1.30–1.45 (m, 2 H), 1.07 (t, *J* = 7.19 Hz, 3

H). HRMS ( $m/z$ ):  $[\text{MH}^+]$  calcd for  $\text{C}_{29}\text{H}_{38}\text{N}_5\text{O}_2$ , 488.3020; found, 488.3016.

**(E)-N-(1-((1*s*,4*s*)-4-(Diethylcarbamoyl)cyclohexyl)-6-(piperidin-1-ylmethyl)-1*H*-benzo[d]imidazol-2(3*H*)-ylidene)benzamide (16).** General procedure A, with diethylamine, was used to produce 16 (35 mg, 63% yield).  $^1\text{H}$  NMR (400 MHz,  $\text{DMSO}-d_6$ )  $\delta$  12.77 (br s, 1 H), 8.30 (m, 2 H), 7.76 (s, 1 H), 7.42–7.57 (m, 4 H), 7.09–7.20 (m, 1 H), 4.73–5.03 (m, 1 H), 3.44–3.59 (m, 1 H), 3.38 (m, 3 H), 2.95–3.01 (m, 2 H), 2.93 (q,  $J = 7.27$  Hz, 4 H), 2.27–2.42 (m, 3 H), 1.89–2.05 (m, 2 H), 1.73–1.89 (m, 2 H), 1.47–1.70 (m, 6 H), 1.32–1.44 (m, 2 H), 1.17 (t,  $J = 7.28$  Hz, 6 H). HRMS ( $m/z$ ):  $[\text{MH}^+]$  calcd for  $\text{C}_{31}\text{H}_{42}\text{N}_5\text{O}_2$ , 516.3333; found, 516.3329.

**(E)-N-(1-((1*s*,4*s*)-4-Carbamoylcyclohexyl)-6-(piperidin-1-ylmethyl)-1*H*-benzo[d]imidazol-2(3*H*)-ylidene)benzamide (17).** General procedure A, with ammonia, was used to produce 17 (20 mg, 40% yield).  $^1\text{H}$  NMR (400 MHz,  $\text{DMSO}-d_6$ )  $\delta$  12.77 (br s, 1 H), 8.17–8.30 (m, 2 H), 7.44–7.54 (m, 5 H), 7.17 (d,  $J = 8.31$  Hz, 1 H), 6.86–6.93 (br s, 2 H), 4.63–4.98 (m, 1 H), 3.42–3.55 (m, 2 H), 2.66–2.84 (m, 2 H), 2.53–2.58 (m, 1 H), 2.26–2.42 (m, 4 H), 2.12–2.25 (m, 2 H), 1.68–1.81 (m, 2 H), 1.59–1.68 (m, 2 H), 1.46–1.57 (m, 4 H), 1.34–1.44 (m, 2 H). HRMS ( $m/z$ ):  $[\text{MH}^+]$  calcd for  $\text{C}_{27}\text{H}_{34}\text{N}_5\text{O}_2$ , 460.2707; found, 460.2712.

**(E)-N-(1-((1*s*,4*s*)-4-(Isopropylcarbamoyl)cyclohexyl)-6-(piperidin-1-ylmethyl)-1*H*-benzo[d]imidazol-2(3*H*)-ylidene)benzamide (18).** General procedure A, with isopropylamine, was used to produce 18 (35 mg, 64% yield).  $^1\text{H}$  NMR (400 MHz,  $\text{DMSO}-d_6$ )  $\delta$  9.93 (s, 1 H), 8.25–8.31 (m, 2 H), 7.91 (s, 1 H), 7.66–7.73 (m, 1 H), 7.61 (d,  $J = 8.22$  Hz, 1 H), 7.44–7.57 (m, 3 H), 7.36–7.43 (m, 1 H), 4.64–4.78 (m, 1 H), 4.28–4.38 (m, 3 H), 4.00–4.14 (m, 1 H), 3.31–3.45 (m, 2 H), 2.76–2.97 (m, 3 H), 2.53–2.61 (m, 1 H), 2.07–2.22 (m, 2 H), 1.75–1.90 (m, 2 H), 1.64–1.76 (m, 4 H), 1.17–1.32 (m, 2 H), 1.10 (d,  $J = 6.55$  Hz, 6 H). HRMS ( $m/z$ ):  $[\text{MH}^+]$  calcd for  $\text{C}_{30}\text{H}_{40}\text{N}_5\text{O}_2$ , 502.3177; found, 502.3183.

**(1*s*,4*s*)-4-((5-(Hydroxymethyl)-2-nitrophenylamino)-*N*-isopropylcyclohexanecarboxamide (20).** To a suspension of 19 (7.09 g, 32.1 mmol) and *N,N*-diisopropylethylamine (15.3 mL, 88 mmol) in acetonitrile (50 mL) was added 4 (5.0 g, 29.2 mmol), and the reaction was stirred overnight at 80 °C. After 16 h, the reaction mixture was cooled to ambient temperature and concentrated. The crude product was purified by column chromatography, eluting with 0–100% ethyl acetate in DCM to provide 20 (7.0 g, 71% yield) as an orange solid.  $^1\text{H}$  NMR (400 MHz,  $\text{DMSO}-d_6$ )  $\delta$  8.35 (d,  $J = 7.5$  Hz, 1 H), 8.04 (d,  $J = 8.9$  Hz, 1 H), 7.57 (d,  $J = 8.0$  Hz, 1 H), 6.99 (s, 1 H), 6.62 (dd,  $J = 1.7$  Hz, 8.9 Hz, 1 H), 5.41 (t,  $J = 5.8$  Hz, 1 H), 4.51 (d,  $J = 5.5$  Hz, 2 H), 3.89–3.96 (m, 1 H), 3.77–3.86 (m, 1 H), 2.16–2.25 (m, 1 H), 1.81–1.89 (m, 2 H), 1.57–1.74 (m, 6 H), 1.03 (d,  $J = 6.5$  Hz, 6 H). LC/MS ( $\text{ESI}^+$ )  $m/z = 336.0$  (M + H).

**4-Fluorobenzoyl Isothiocyanate (21).** To a suspension of potassium thiocyanate (16.2 g, 167 mmol) in acetone (93 mL) was added 4-fluorobenzoyl chloride (16.4 mL, 139 mmol) dropwise, and the reaction was stirred for 7 h at 50 °C. After the reaction was complete, the reaction mixture was cooled to ambient temperature and filtered through a pad of Celite. The filtrate was concentrated, and the residue was dissolved in DCM (25 mL) and passed through a silica gel pad, eluting with 1:1 hexanes/DCM. The product fractions were combined and concentrated to produce 21 (11.1 g, 44% yield) as an orange liquid that solidified upon standing.  $^1\text{H}$  NMR (400 MHz,  $\text{CDCl}_3$ )  $\delta$  8.10 (dd,  $J = 5.3$  Hz, 9.0 Hz, 2 H), 7.18 (dd,  $J = 8.2$  Hz, 9.0 Hz, 2 H).

**(E)-4-Fluoro-N-(6-(hydroxymethyl)-1-((1*s*,4*s*)-4-(isopropylcarbamoyl)cyclohexyl)-1*H*-benzo[d]imidazol-2(3*H*)-ylidene)benzamide (22).** Step 1: To a solution of 20 (2.0 g, 5.96 mmol) in ethanol (25 mL) was added 10% (w/w) palladium on carbon (0.635 g, 0.596 mmol). A hydrogen balloon was installed, and the reaction was stirred under a hydrogen atmosphere for 3 h. After 3 h, the reaction mixture was filtered through a Celite pad and concentrated to produce (1*s*,4*s*)-4-(2-amino-5-(hydroxymethyl)phenylamino)-*N*-isopropylcyclohexanecarboxamide as a brown oil.

Step 2: To a solution of the crude (1*s*,4*s*)-4-(2-amino-5-(hydroxymethyl)phenylamino)-*N*-isopropylcyclohexanecarboxamide in tetrahydrofuran (30 mL) at 0 °C was added 21 (1.30 g, 7.15 mmol),

and the reaction was stirred at 0 °C for 15 min. After 15 min, *N,N*-diisopropylethylamine (1.56 mL, 8.94 mmol) and 1-(3-dimethylaminopropyl)-3-ethylcarbodiimide hydrochloride (1.71 g, 8.94 mmol) were added, and the reaction was stirred for 2 h at 60 °C and then overnight at ambient temperature. The reaction mixture was concentrated, and the residue was partitioned between water and DCM. The organic layer was dried over anhydrous magnesium sulfate, filtered, and concentrated. The crude product was purified by column chromatography, eluting with 0–100% ethyl acetate in DCM, to produce 22 (2.14 g, 80% yield over two steps) as a tan solid.  $^1\text{H}$  NMR (400 MHz,  $\text{DMSO}-d_6$ )  $\delta$  12.75 (s, 1 H), 8.33 (dd,  $J = 5.9$  Hz, 8.8 Hz, 2 H), 7.63 (d,  $J = 7.9$  Hz, 1 H), 7.58 (s, 1 H), 7.49 (d,  $J = 8.2$  Hz, 1 H), 7.13–7.28 (m, 3 H), 5.20 (t,  $J = 5.6$  Hz, 1 H), 4.75–4.86 (m, 1 H), 4.56 (d,  $J = 5.6$  Hz, 2 H), 3.99–4.09 (m, 1 H), 2.71–2.84 (m, 2 H), 2.53–2.59 (m, 1 H), 2.10–2.20 (m, 2 H), 1.67–1.79 (m, 2 H), 1.57–1.67 (m, 2 H), 1.10 (d,  $J = 6.6$  Hz, 6 H). LC/MS ( $\text{ESI}^+$ )  $m/z = 453.0$  (M + H).

**(E)-4-Fluoro-N-(1-((1*s*,4*s*)-4-(isopropylcarbamoyl)cyclohexyl)-1*H*-benzo[d]imidazol-2(3*H*)-ylidene)benzamide (24).** Step 1: In an analogous sequence to the reactions described for 20, 8, and 9, 4-chloro-2-fluoro-1-nitrobenzene (159 mg, 0.91 mmol) was converted to (1*s*,4*s*)-4-(2-amino-1*H*-benzo[d]imidazol-1-yl)-*N*-isopropylcyclohexanecarboxamide (162 mg, 60% yield for three steps). LC/MS ( $\text{ESI}^+$ )  $m/z = 300.9$  (M + H).

Step 2: To a solution of (1*s*,4*s*)-4-(2-amino-1*H*-benzo[d]imidazol-1-yl)-*N*-isopropylcyclohexanecarboxamide (162 mg, 0.54 mmol) and pyridine (87  $\mu\text{L}$ , 1.08 mmol) in DCM (5 mL) at 0 °C was added 4-fluorobenzoyl chloride (64  $\mu\text{L}$ , 0.54 mmol). The reaction was allowed to warm to ambient temperature and stirred overnight. The reaction mixture was concentrated and purified by column chromatography, eluting with 20–100% ethyl acetate in hexanes, to produce 24 (62 mg, 27% yield) as an off-white solid.  $^1\text{H}$  NMR (400 MHz,  $\text{DMSO}-d_6$ )  $\delta$  12.79 (br s, 1 H), 8.28–8.35 (m, 2 H), 7.69 (d,  $J = 6.8$  Hz, 2 H), 7.54–7.58 (m, 1 H), 7.18–7.28 (m, 4 H), 4.82–4.96 (m, 1 H), 3.95–4.06 (m, 1 H), 2.71–2.84 (m, 2 H), 2.52–2.57 (m, 1 H), 2.04–2.14 (m, 2 H), 1.67–1.79 (m, 2 H), 1.57–1.67 (m, 2 H), 1.10 (d,  $J = 6.5$  Hz, 6 H). HRMS ( $m/z$ ):  $[\text{MH}^+]$  calcd for  $\text{C}_{24}\text{H}_{27}\text{FN}_4\text{O}_2$ , 423.2191; found, 423.2193.

**(E)-4-Fluoro-N-(1-((1*s*,4*s*)-4-(isopropylcarbamoyl)cyclohexyl)-6-(piperidin-1-ylmethyl)-1*H*-benzo[d]imidazol-2(3*H*)-ylidene)benzamide (25).** 25 (40 mg, 73.7% yield) was prepared from 9 using the reaction sequence described for 18, substituting 4-fluorobenzoyl chloride for benzoyl chloride.  $^1\text{H}$  NMR (400 MHz,  $\text{DMSO}-d_6$ )  $\delta$  10.54 (s, 1 H), 8.32–8.47 (m, 2 H), 8.01 (s, 1 H), 7.76 (d,  $J = 7.73$  Hz, 1 H), 7.64 (d,  $J = 8.22$  Hz, 1 H), 7.47–7.53 (m, 1 H), 7.25–7.34 (m, 2 H), 4.63–4.82 (m, 1 H), 4.29–4.44 (m, 2 H), 4.05–4.19 (m, 1 H), 3.89–4.03 (m, 1 H), 3.33–3.47 (m, 2 H), 2.84–3.03 (m, 4 H), 2.59–2.64 (m, 1 H), 2.12–2.25 (m, 2 H), 1.81–1.89 (m, 3 H), 1.68–1.79 (m, 4 H), 1.27–1.34 (m, 2 H), 1.15 (d,  $J = 6.55$  Hz, 6 H). HRMS ( $m/z$ ):  $[\text{MH}^+]$  calcd for  $\text{C}_{30}\text{H}_{39}\text{FN}_5\text{O}_2$ , 520.3082; found, 520.3084.

**Preparation of 26, 29–30, and 34–40. General Procedure B.** To a solution of 22 (100 mg, 0.221 mmol) in DCM (2.5 mL) at 0 °C was added thionyl chloride (81  $\mu\text{L}$ , 1.11 mmol) dropwise, and the reaction was stirred at 0 °C for 30 min. After 30 min, the reaction mixture was concentrated and dried in vacuo. To a suspension of the crude intermediate in acetonitrile (2 mL) was added an amine, and the reaction was stirred overnight at ambient temperature. After 16 h, the reaction was concentrated and the crude product was purified by reverse-phase preparative HPLC using a gradient of 15–90% [0.1% TFA in acetonitrile] in [0.1% TFA in water], to provide the desired product.

**(E)-N-(6-((1,1-Dioxidothiomorpholino)methyl)-1-((1*s*,4*s*)-4-(isopropylcarbamoyl)cyclohexyl)-1*H*-benzo[d]imidazol-2(3*H*)-ylidene)-4-fluorobenzamide (26).** General procedure B, with thiomorpholine 1,1-dioxide (TCI America, 299 mg, 2.21 mmol), was used to produce 26 (67 mg, 53.2% yield) as a light-yellow solid.  $^1\text{H}$  NMR (400 MHz,  $\text{DMSO}-d_6$ )  $\delta$  12.75 (s, 1 H), 8.31 (dd,  $J = 6.2$  Hz, 8.7 Hz, 2 H), 7.80 (s, 1 H), 7.68 (d,  $J = 7.8$  Hz, 1 H), 7.49 (d,  $J = 8.2$  Hz, 1 H), 7.25 (dd,  $J = 8.6$  Hz, 8.6 Hz, 2 H), 7.13, (d,  $J = 8.6$  Hz, 1 H),

4.86–4.97 (m, 1 H), 4.00–4.07 (m, 1 H), 3.76 (s, 2 H), 3.18–3.25 (m, 4 H), 2.88–2.96 (m, 4 H), 2.72–2.86 (m, 2 H), 2.53–2.60 (m, 1 H), 2.05–2.14 (m, 2 H), 1.69–1.79 (m, 2 H), 1.59–1.65 (m, 2 H), 1.21–1.30 (m, 1H), 1.11 (d,  $J = 6.6$  Hz, 6 H). HRMS ( $m/z$ ):  $[\text{MH}^+]$  calcd for  $\text{C}_{29}\text{H}_{37}\text{FN}_5\text{O}_3$ , 570.2545; found, 570.2545.

**(E)-N-(6-((1*H*-1,2,4-Triazol-1-yl)methyl)-1-((1*s*,4*s*)-4-(isopropylcarbamoyl)cyclohexyl)-1*H*-benzo[d]imidazol-2(3*H*)-ylidene)-4-fluorobenzamide (27).** To a solution of **22** (100 mg, 0.221 mmol) in DCM (2.5 mL) at 0 °C was added thionyl chloride (81  $\mu\text{L}$ , 1.11 mmol) dropwise, and the reaction was stirred at 0 °C for 30 min. After 30 min, the reaction mixture was concentrated and dried in vacuo. The residue was suspended in acetonitrile (2 mL) and cooled to 0 °C. To the suspension were added 1,2,4-triazole (153 mg, 2.21 mmol), potassium carbonate (305 mg, 2.21 mmol), and sodium iodide (33.1 mg, 0.221 mmol), and the reaction was allowed to warm to ambient temperature. After 16 h, the reaction mixture was partitioned between water and DCM; the aqueous layer was acidified to pH 8 with 1 N aqueous HCl and extracted with DCM. The combined organic layers were concentrated, adsorbed onto a silica gel loading column, and purified by column chromatography, eluting with 0–10% methanol in DCM to produce **27** (35 mg, 31.5% yield) as a light-yellow solid.  $^1\text{H}$  NMR (400 MHz,  $\text{DMSO}-d_6$ )  $\delta$  12.80 (s, 1 H), 8.69 (s, 1 H), 8.33 (dd,  $J = 6.0$  Hz, 8.6 Hz, 2 H), 7.95 (s, 1 H), 7.76 (s, 1 H), 7.67 (d,  $J = 7.6$  Hz, 1 H), 7.50 (d,  $J = 8.1$  Hz, 1 H), 7.24 (dd,  $J = 8.8$  Hz, 8.8 Hz, 2 H), 7.15 (d,  $J = 8.2$  Hz, 1 H), 5.45 (s, 2 H), 4.72–4.84 (m, 1 H), 4.03–4.13 (m, 1 H), 2.71–2.87 (m, 2 H), 2.52–2.57 (m, 1 H), 2.06–2.17 (m, 2 H), 1.66–1.79 (m, 2 H), 1.55–1.65 (m, 2 H), 1.21–1.30 (m, 1H), 1.11 (d,  $J = 6.6$  Hz, 6 H). HRMS ( $m/z$ ):  $[\text{MH}^+]$  calcd for  $\text{C}_{27}\text{H}_{31}\text{FN}_5\text{O}_2$ , 504.2518; found, 504.2517.

**(E)-4-Fluoro-N-(1-((1*s*,4*s*)-4-(isopropylcarbamoyl)cyclohexyl)-6-(pyridin-2-yl)oxy)-1*H*-benzo[d]imidazol-2(3*H*)-ylidene)benzamide (28).** Step 1: To a solution of 3-fluoro-4-nitrophenol (2.96 g, 18.8 mmol) in DMF (18.8 mL) was added 1-(chloromethyl)-4-methoxybenzene (2.55 mL, 18.8 mmol) and potassium carbonate (5.20 g, 37.6 mmol), and the reaction was stirred overnight at ambient temperature. After 16 h, the reaction mixture was partitioned between water and ethyl acetate, and the aqueous layer was extracted with ethyl acetate. The combined organic layers were washed with 1 N aqueous sodium hydroxide and brine, dried over anhydrous sodium sulfate, filtered, and concentrated. The residue was triturated with ether produce 2-fluoro-4-(4-methoxybenzyloxy)-1-nitrobenzene (4.39 g, 84% yield).

Step 2: 2-Fluoro-4-(4-methoxybenzyloxy)-1-nitrobenzene (507 mg, 1.83 mmol) and **19** (404 mg, 1.83 mmol) were converted to (1*s*,4*s*)-*N*-isopropyl-4-((5-((4-methoxybenzyl)oxy)-2-nitrophenyl)amino)cyclohexanecarboxamide (476 mg, 59.0% yield) as described for **20**. LC/MS ( $\text{ESI}^+$ )  $m/z = 442.2$  (M + H).

Step 3: To a solution of (1*s*,4*s*)-*N*-isopropyl-4-((5-((4-methoxybenzyl)oxy)-2-nitrophenyl)amino)cyclohexanecarboxamide (452 mg, 1.02 mmol) in methanol (5.1 mL) was added acetic acid (0.29 mL, 5.12 mmol) and zinc (669 mg, 10.2 mmol), and the mixture was stirred at ambient temperature for 3 h. The reaction was filtered through a pad of Celite, and the filtrate was concentrated to produce (1*s*,4*s*)-4-(2-amino-5-(4-methoxybenzyloxy)phenylamino)-*N*-isopropylcyclohexanecarboxamide (421 mg, quantitative yield). LC/MS ( $\text{ESI}^+$ )  $m/z = 412.2$  (M + H).

Step 4: To a solution of (1*s*,4*s*)-4-(2-amino-5-(4-methoxybenzyloxy)phenylamino)-*N*-isopropylcyclohexanecarboxamide (400 mg, 0.97 mmol) in ethanol (4.9 mL) was added cyanogen bromide (165 mg, 1.55 mmol), and the reaction was stirred at ambient temperature for 2 h. The reaction mixture was concentrated, and the residue was redissolved in DCM (10 mL), washed with water, 1 N aqueous sodium hydroxide, and brine. The organic layer was dried over anhydrous sodium sulfate, filtered, and concentrated to produce (1*s*,4*s*)-4-(2-amino-6-((4-methoxybenzyloxy)-1*H*-benzo[d]imidazol-1-yl)-*N*-isopropylcyclohexanecarboxamide. LC/MS ( $\text{ESI}^+$ )  $m/z = 437.2$  (M + H).

Step 5: To a solution of (1*s*,4*s*)-4-(2-amino-6-((4-methoxybenzyloxy)-1*H*-benzo[d]imidazol-1-yl)-*N*-isopropylcyclohexanecarboxamide (424 mg, 0.97 mmol) and 4-fluorobenzoyl chloride (0.17 mL, 1.46

mmol) in DCM was added triethylamine (0.27 mL, 1.94 mmol), and the reaction was stirred at ambient temperature for 10 min. The reaction mixture was then diluted with DCM, washed with water and brine, and concentrated. After column chromatography, eluting with 0–10% methanol in DCM, a mixture of the mono- and bis-acylated products, in an approximately 2:1 ratio, was obtained.

The mixture of products was redissolved in methanol (3.25 mL) and 1,4-dioxane (3.25 mL) and treated with sodium hydroxide (47 mg, 1.17 mmol). After 1 h, the reaction mixture was diluted with DCM, washed with 1 N aqueous sodium hydroxide and brine, and concentrated. The residue was purified by column chromatography, eluting with 0–50% ethyl acetate in hexanes, to produce (E)-4-fluoro-*N*-(1-((1*s*,4*s*)-4-(isopropylcarbamoyl)cyclohexyl)-6-((4-methoxybenzyl)oxy)-1*H*-benzo[d]imidazol-2(3*H*)-ylidene)benzamide (275 mg, 51% yield). LC/MS ( $\text{ESI}^+$ )  $m/z = 559.2$  (M + H).

Step 6: To a solution of (E)-4-fluoro-*N*-(1-((1*s*,4*s*)-4-(isopropylcarbamoyl)cyclohexyl)-6-((4-methoxybenzyl)oxy)-1*H*-benzo[d]imidazol-2(3*H*)-ylidene)benzamide (232 mg, 0.42 mmol) in DCM was added trifluoroacetic acid (96  $\mu\text{L}$ , 1.25 mmol), and the reaction was stirred at ambient temperature for 90 min. Another portion of trifluoroacetic acid (96  $\mu\text{L}$ , 1.25 mmol) was added, and the reaction was stirred at ambient temperature for an additional hour. The reaction was then partitioned between DCM and 1 N aqueous sodium hydroxide. The aqueous layer was washed with DCM, and the pH was adjusted to about 8 with 6 N aqueous HCl and saturated aqueous ammonium chloride. The resulting precipitate was collected by vacuum filtration, washed with water, and dried in vacuo to produce (E)-4-fluoro-*N*-(6-hydroxy-1-((1*s*,4*s*)-4-(isopropylcarbamoyl)cyclohexyl)-1*H*-benzo[d]imidazol-2(3*H*)-ylidene)benzamide. LC/MS ( $\text{ESI}^+$ )  $m/z = 439.2$  (M + H).

To a solution of (E)-4-fluoro-*N*-(6-hydroxy-1-((1*s*,4*s*)-4-(isopropylcarbamoyl)cyclohexyl)-1*H*-benzo[d]imidazol-2(3*H*)-ylidene)benzamide and cesium carbonate (166 mg, 0.511 mmol) in NMP (0.6 mL) in a microwave vial was added 2-chloropyridine (0.036 mL, 0.383 mmol), and the reaction was irradiated for 6 h at 160 °C in a Biotage Initiator microwave. The reaction mixture was partitioned between water and ethyl acetate, and the aqueous layer was extracted with ethyl acetate. The combined organic layers were washed with brine, dried over anhydrous sodium sulfate, filtered, and concentrated. The crude product was purified by preparative HPLC, using a gradient of 10–90% [0.1% TFA in acetonitrile] in [0.1% TFA in water]. The product fractions were partitioned between saturated aqueous sodium bicarbonate and 5% 2-propanol in DCM. The organic layer was washed with brine, dried over anhydrous sodium sulfate, filtered, and concentrated to produce **28** (32 mg, 35% yield) as an off-white solid.  $^1\text{H}$  NMR (400 MHz,  $\text{DMSO}-d_6$ )  $\delta$  12.81 (s, 1 H), 8.27–8.38 (m, 2 H), 8.07–8.19 (m, 1 H), 7.80–7.90 (m, 1 H), 7.51–7.62 (m, 2 H), 7.48 (d,  $J = 2.05$  Hz, 1 H), 7.20–7.29 (m, 2 H), 7.00–7.18 (m, 1 H), 6.97 (dd,  $J = 8.56$  Hz, 2.10 Hz, 1 H), 6.95–7.10 (m, 1 H), 4.80–4.95 (m, 1 H), 3.75–3.93 (m, 1 H), 2.56–2.77 (m, 2 H), 2.42–2.56 (m, 1 H), 2.01–2.14 (m, 2 H), 1.54–1.82 (m, 4 H), 0.98 (d,  $J = 8.00$  Hz, 6 H). HRMS ( $m/z$ ):  $[\text{MH}^+]$  calcd for  $\text{C}_{29}\text{H}_{31}\text{FN}_5\text{O}_3$ , 516.2405; found, 516.2410.

**(E)-4-Fluoro-N-(1-((1*s*,4*s*)-4-(isopropylcarbamoyl)cyclohexyl)-6-(piperazin-1-ylmethyl)-1*H*-benzo[d]imidazol-2(3*H*)-ylidene)benzamide (29).** General procedure B, with piperazine (190 mg, 2.21 mmol), was used to produce **29** (58 mg, 50.4% yield) as a white solid.  $^1\text{H}$  NMR (400 MHz,  $\text{DMSO}-d_6$ )  $\delta$  8.30 (dd,  $J = 5.8$  Hz, 8.8 Hz, 2 H), 7.67 (d,  $J = 7.9$  Hz, 1 H), 7.61 (s, 1 H), 7.48 (d,  $J = 8.2$  Hz, 1 H), 7.24 (dd,  $J = 8.8$  Hz, 9.0 Hz, 2 H), 7.15 (d,  $J = 8.1$  Hz, 1 H), 4.79–4.92 (m, 1 H), 3.98–4.10 (m, 1 H), 3.55 (s, 2 H), 2.80–2.91 (m, 2 H), 2.64–2.79 (m, 2 H), 2.53–2.57 (m, 1 H), 2.34–2.44 (m, 4 H), 2.09–2.19 (m, 2 H), 1.55–1.79 (m, 4 H), 1.21–1.30 (m, 1 H), 1.11 (d,  $J = 6.6$  Hz, 6 H). HRMS ( $m/z$ ):  $[\text{MH}^+]$  calcd for  $\text{C}_{29}\text{H}_{38}\text{FN}_6\text{O}_2$ , 521.3035; found, 521.3034.

**(E)-4-Fluoro-N-(1-((1*s*,4*s*)-4-(isopropylcarbamoyl)cyclohexyl)-6-((3-oxopiperazin-1-yl)methyl)-1*H*-benzo[d]imidazol-2(3*H*)-ylidene)benzamide (30).** General procedure B, with piperazin-2-one (221 mg, 2.21 mmol), was used to produce **30** (72 mg, 50.3% yield) as a white solid.  $^1\text{H}$  NMR (400 MHz,  $\text{DMSO}-d_6$ )

$\delta$  12.79 (br, 1 H), 8.26–8.38 (m, 2 H), 7.65 (d,  $J = 7.5$  Hz, 1 H), 7.69–7.82 (m, 1 H), 7.49–7.60 (m, 2 H), 7.13–7.30 (m, 3 H), 4.73–4.91 (m, 1 H), 3.98–4.10 (m, 1 H), 3.54–3.63 (m, 2 H), 3.12–3.26 (m, 2 H), 2.65–3.03 (m, 4 H), 2.53–2.61 (m, 1 H), 2.09–2.20 (m, 2 H), 1.57–1.79 (m, 4 H), 1.11 (d,  $J = 6.7$  Hz, 6 H). HRMS ( $m/z$ ):  $[\text{MH}^+]$  calcd for  $\text{C}_{29}\text{H}_{36}\text{FN}_5\text{O}_3$ , 535.2827; found, 535.2827.

**(E)-N-(6-((4-(Aminomethyl)piperidin-1-yl)methyl)-1-((1*S*,4*S*)-4-(isopropylcarbamoyl)cyclohexyl)-1*H*-benzo[d]imidazol-2(3*H*)-ylidene)-4-fluorobenzamide (31).** Step 1: Using the reaction sequence described for the synthesis of **25**, substituting *tert*-butyl piperidine-4-ylcarbamate (Matrix Scientific) for piperidine, **9** (400 mg, 0.94 mmol) was converted to *tert*-butyl ((1-(((*E*)-2-((4-fluorobenzoyl)imino)-3-((1*S*,4*S*)-4-(isopropylcarbamoyl)cyclohexyl)-2,3-dihydro-1*H*-benzo[d]imidazol-5-yl)methyl)piperidin-4-yl)methyl)piperidin-4-yl)methyl)carbamate.

Step 2: The *tert*-butyl ((1-(((*E*)-2-((4-fluorobenzoyl)imino)-3-((1*S*,4*S*)-4-(isopropylcarbamoyl)cyclohexyl)-2,3-dihydro-1*H*-benzo[d]imidazol-5-yl)methyl)piperidin-4-yl)methyl)carbamate was suspended in a solution of 4 M HCl in 1,4-dioxane (23.5 mL, 94 mmol), and the reaction was stirred at ambient temperature overnight. After 16 h, the reaction mixture was concentrated. The residue was resuspended in DCM, washed with aqueous sodium bicarbonate, and concentrated. The crude product was purified by column chromatography, eluting with 10–100% [9:1 DCM/methanol with 1% ammonium hydroxide] in [0.1% ammonium hydroxide in DCM] to produce **31** (300 mg, 58% yield over two steps).  $^1\text{H}$  NMR (400 MHz,  $\text{DMSO}-d_6$ )  $\delta$  8.31 (dd,  $J = 4.9$  Hz, 8.9 Hz, 2 H), 7.64 (d,  $J = 7.4$  Hz, 1 H), 7.58 (s, 1 H), 7.47 (d,  $J = 8.1$  Hz, 1 H), 7.24 (dd,  $J = 8.9$  Hz, 8.9 Hz, 2 H), 7.14 (dd,  $J = 1.2$  Hz, 8.2 Hz, 1 H), 4.79–4.92 (m, 1 H), 3.80–4.09 (m, 1 H), 3.51 (s, 2 H), 2.65–2.88 (m, 4 H), 2.52–2.56 (m, 1 H), 2.45 (d,  $J = 5.9$  Hz, 1 H), 2.09–2.19 (m, 2 H), 1.84–1.93 (m, 2 H), 1.54–1.78 (m, 6 H), 1.13–1.35 (m, 5 H), 1.11 (d,  $J = 6.7$  Hz, 6 H). HRMS ( $m/z$ ):  $[\text{MH}^+]$  calcd for  $\text{C}_{31}\text{H}_{43}\text{FN}_5\text{O}_2$ , 549.3348; found, 549.3352.

**1-(((E)-2-((4-Fluorobenzoyl)imino)-3-((1*S*,4*S*)-4-(isopropylcarbamoyl)cyclohexyl)-2,3-dihydro-1*H*-benzo[d]imidazol-5-yl)methyl)piperidine-2-carboxylic acid hydrochloride (32).** Step 1: To a suspension of *tert*-butyl piperidine-2-carboxylate hydrochloride (AstaTech, Inc., 229 mg, 1.38 mmol) in DCM (5 mL) was added 1 N aqueous sodium hydroxide (1.38 mL, 1.38 mmol), and the mixture was shaken. The layers were separated, and the organic layer was dried over anhydrous sodium sulfate, filtered, and concentrated to produce *tert*-butyl piperidine-2-carboxylate.

Step 2: To a suspension of **22** (0.042 g, 0.093 mmol) in DCM (1 mL) at 0 °C was added thionyl chloride (0.11 g, 0.93 mmol), and the reaction was stirred at ambient temperature for 30 min. After 30 min, the reaction mixture was concentrated and dried in vacuo. The residue was suspended in DMSO (2 mL), and *tert*-butyl piperidine-2-carboxylate (100 mg, 0.538 mmol) was added. The reaction was stirred at ambient temperature for 2 h, diluted with water (2 mL), and extracted with DCM (10 mL). The organic layer was dried over anhydrous sodium sulfate, filtered, and concentrated. The crude ester was purified by preparative HPLC, using a gradient of 10–70% [0.1% TFA in acetonitrile] in [0.1% TFA in water]. The product fractions were combined and concentrated to produce *tert*-butyl 1-(((*E*)-2-((4-fluorobenzoyl)imino)-3-((1*S*,4*S*)-4-(isopropylcarbamoyl)cyclohexyl)-2,3-dihydro-1*H*-benzo[d]imidazol-5-yl)methyl)piperidine-2-carboxylate, which was then dissolved in 4 M HCl in 1,4-dioxane (1.16 mL, 4.64 mmol) and stirred for 16 h at ambient temperature. The reaction mixture was concentrated and dried in vacuo to produce **32** (20 mg, 35.9% yield).  $^1\text{H}$  NMR (400 MHz,  $\text{DMSO}-d_6$ )  $\delta$  10.09 (br s, 1 H), 8.34 (dd,  $J = 5.9$  Hz, 8.6 Hz, 2 H), 7.82 (s, 1 H), 7.72 (d,  $J = 7.5$  Hz, 1 H), 7.61 (d,  $J = 8.3$  Hz, 1 H), 7.21–7.34 (m, 3 H), 4.62–4.77 (m, 1 H), 4.41–4.59 (m, 1 H), 4.20–4.30 (m, 3 H), 3.97–4.11 (m, 1 H), 3.35–3.44 (m, 1 H), 3.00–3.13 (m, 1 H), 2.78–2.96 (m, 2 H), 2.53–2.59 (m, 1 H), 2.06–2.27 (m, 3 H), 1.59–1.85 (m, 8 H), 1.42–1.59 (m, 1 H), 1.09 (d,  $J = 6.6$  Hz, 6 H). HRMS ( $m/z$ ):  $[\text{MH}^+]$  calcd for  $\text{C}_{31}\text{H}_{39}\text{FN}_5\text{O}_4$ , 564.2981; found, 564.2978.

**1-(((E)-2-((4-Fluorobenzoyl)imino)-3-((1*S*,4*S*)-4-(isopropylcarbamoyl)cyclohexyl)-2,3-dihydro-1*H*-benzo[d]imidazol-5-yl)methyl)piperidine-4-carboxylic acid hydrochloride (33).** **33** (20 mg, 24.3% yield) was prepared according to the

procedures in **32**, substituting *tert*-butyl piperidine-4-carboxylate hydrochloride (0.229 g, 1.38 mmol) for *tert*-butyl piperidine-2-carboxylate hydrochloride.  $^1\text{H}$  NMR (400 MHz,  $\text{DMSO}-d_6$ )  $\delta$  10.05 (br s, 1 H), 8.31–8.38 (m, 2 H), 7.78–7.93 (m, 1 H), 7.69 (d,  $J = 7.5$  Hz, 1 H), 7.59 (d,  $J = 8.2$  Hz, 1 H), 7.24 (dd,  $J = 8.7$  Hz, 8.7 Hz, 2 H), 4.62–4.75 (m, 1 H), 4.30–4.41 (m, 2 H), 4.00–4.10 (m, 1 H), 3.65–3.74 (m, 1 H), 3.41–3.50 (m, 1 H), 2.82–3.05 (m, 3 H), 2.56–2.62 (m, 1 H), 1.93–2.18 (m, 4 H), 1.54–1.89 (m, 4 H), 1.19–1.32 (m, 2 H), 1.09 (d,  $J = 6.6$  Hz, 6 H). HRMS ( $m/z$ ):  $[\text{MH}^+]$  calcd for  $\text{C}_{31}\text{H}_{39}\text{FN}_5\text{O}_4$ , 564.2981; found, 564.2985.

**1-(((E)-2-((4-Fluorobenzoyl)imino)-3-((1*S*,4*S*)-4-(isopropylcarbamoyl)cyclohexyl)-2,3-dihydro-1*H*-benzo[d]imidazol-5-yl)methyl)piperidine-4-carboxamide (34).** General procedure B, with piperidine-4-carboxamide (283 mg, 2.21 mmol), was used to produce **34** (57 mg, 46.0% yield) as a white solid.  $^1\text{H}$  NMR (400 MHz,  $\text{DMSO}-d_6$ )  $\delta$  12.96 (br s, 1 H), 8.32 (dd,  $J = 6.1$  Hz, 14.2 Hz, 2 H), 8.10 (d,  $J = 6.8$  Hz, 1 H), 7.54–7.70 (m, 2 H), 7.37–7.47 (m, 1 H), 7.26 (dd,  $J = 6.7$  Hz, 8.8 Hz, 2 H), 4.72–4.97 (m, 3 H), 3.59–3.72 (m, 2 H), 3.37–3.52 (m, 2 H), 3.16–3.27 (m, 1 H), 2.71–2.94 (m, 2 H), 2.41–2.48 (m, 1 H), 2.21–2.35 (m, 2 H), 1.89–2.02 (m, 2 H), 1.53–1.80 (m, 5 H), 1.07–1.15 (m, 3 H), 0.75–0.89 (m, 6 H). HRMS ( $m/z$ ):  $[\text{MH}^+]$  calcd for  $\text{C}_{31}\text{H}_{40}\text{FN}_5\text{O}_3$ , 563.3140; found, 563.3144.

**(S)-1-(((E)-2-((4-Fluorobenzoyl)imino)-3-((1*S*,4*R*)-4-(isopropylcarbamoyl)cyclohexyl)-2,3-dihydro-1*H*-benzo[d]imidazol-5-yl)methyl)pyrrolidine-2-carboxamide (35).** General procedure B, with (*S*)-pyrrolidine-2-carboxamide (Bachem AG, 252 mg, 2.21 mmol), was used to produce **35** (41 mg, 33.9% yield) as a white solid.  $^1\text{H}$  NMR (400 MHz,  $\text{DMSO}-d_6$ )  $\delta$  12.73 (br s, 1 H), 8.31 (dd,  $J = 5.8$  Hz, 8.8 Hz, 2 H), 7.92 (s, 1 H), 7.74 (d,  $J = 7.7$  Hz, 1 H), 7.25 (dd,  $J = 8.9$  Hz, 8.9 Hz, 2 H), 7.43–7.53 (m, 2 H), 7.14 (d,  $J = 8.2$  Hz, 1 H), 7.01–7.07 (m, 1 H), 4.87–4.99 (m, 1 H), 3.92–4.06 (m, 2 H), 3.42–3.49 (m, 1 H), 2.87–3.00 (m, 2 H), 2.65–2.79 (m, 1 H), 2.53–2.59 (m, 1 H), 2.01–2.27 (m, 4 H), 1.56–1.83 (m, 8 H), 1.07–1.13 (m, 6 H). HRMS ( $m/z$ ):  $[\text{MH}^+]$  calcd for  $\text{C}_{30}\text{H}_{37}\text{FN}_5\text{O}_3$ , 549.2984; found, 549.2982.

**(E)-4-Fluoro-N-(6-((4-(2-hydroxypropan-2-yl)piperidin-1-yl)methyl)-1-((1*S*,4*S*)-4-(isopropylcarbamoyl)cyclohexyl)-1*H*-benzo[d]imidazol-2(3*H*)-ylidene)benzamide (36).** General procedure B, with **23** (TCI America, 200 mg, 1.39 mmol), was used to produce **36** (77 mg, 60.3% yield) as a white solid.  $^1\text{H}$  NMR (400 MHz,  $\text{DMSO}-d_6$ )  $\delta$  12.75 (br s, 1 H), 8.32 (dd,  $J = 6.0$  Hz, 8.6 Hz, 2 H), 7.63 (d,  $J = 7.7$  Hz, 1 H), 7.57 (s, 1 H), 7.48 (d,  $J = 7.9$  Hz, 1 H), 7.24 (dd,  $J = 8.8$  Hz, 8.8 Hz, 2 H), 7.16 (d,  $J = 7.8$  Hz, 1 H), 4.76–4.91 (m, 1 H), 4.00–4.08 (m, 2 H), 3.43–3.58 (m, 2 H), 2.82–2.98 (m, 2 H), 2.65–2.80 (m, 2 H), 2.54–2.57 (m, 1 H), 2.11–2.20 (m, 2 H), 1.78–1.90 (m, 2 H), 1.59–1.78 (m, 6 H), 1.18–1.33 (m, 3 H), 1.11 (d,  $J = 6.6$  Hz, 6 H), 1.02 (s, 6 H). HRMS ( $m/z$ ):  $[\text{MH}^+]$  calcd for  $\text{C}_{33}\text{H}_{45}\text{FN}_5\text{O}_3$ , 578.3428; found, 578.3493.

**(E)-4-Fluoro-N-(6-(((S)-2-(2-hydroxypropan-2-yl)pyrrolidin-1-yl)methyl)-1-((1*S*,4*R*)-4-(isopropylcarbamoyl)cyclohexyl)-1*H*-benzo[d]imidazol-2(3*H*)-ylidene)benzamide (37).** General procedure B, with a premixed solution of (*S*)-2-(pyrrolidin-2-yl)propan-2-ol hydrochloride<sup>23</sup> (183 mg, 1.11 mmol) and sodium hydride (60% dispersion in mineral oil, 44 mg, 1.11 mmol) in acetonitrile (2 mL), was used to produce **37** (44 mg, 35.3% yield) as a dark solid.  $^1\text{H}$  NMR (400 MHz,  $\text{DMSO}-d_6$ )  $\delta$  12.71 (s, 1 H), 8.30 (dd,  $J = 5.9$  Hz, 8.9 Hz, 2 H), 7.79 (s, 1 H), 7.70 (d,  $J = 8.0$  Hz, 1 H), 7.46 (d,  $J = 8.0$  Hz, 1 H), 7.22–7.29 (m, 2 H), 7.18 (d,  $J = 8.0$  Hz, 1 H), 4.86–4.96 (m, 1 H), 4.36 (d,  $J = 13.3$  Hz, 1 H), 4.14 (s, 1 H), 3.98–4.09 (m, 1 H), 3.51 (d,  $J = 14.4$  Hz, 1 H), 2.76–2.90 (m, 3 H), 2.62–2.68 (m, 1 H), 2.52–2.57 (m, 1 H), 2.19–2.28 (m, 1 H), 2.07–2.13 (m, 2 H), 1.55–1.81 (m, 8 H), 1.14 (s, 6 H), 1.09 (d,  $J = 6.6$  Hz, 6 H). HRMS ( $m/z$ ):  $[\text{MH}^+]$  calcd for  $\text{C}_{32}\text{H}_{42}\text{FN}_5\text{O}_3$ , 564.3344; found, 564.3342.

**(E)-4-Fluoro-N-(6-((3-(2-hydroxypropan-2-yl)pyrrolidin-1-yl)methyl)-1-((1*S*,4*S*)-4-(isopropylcarbamoyl)cyclohexyl)-1*H*-benzo[d]imidazol-2(3*H*)-ylidene)benzamide (38).** General procedure B, with 2-(pyrrolidin-3-yl)propan-2-ol hydrochloride<sup>24</sup> (110 mg, 0.66 mmol) and triethylamine (0.15 mL, 1.11 mmol), was used to produce **38** (65 mg, 52.2% yield) as a light-yellow solid.  $^1\text{H}$  NMR (400 MHz,  $\text{DMSO}-d_6$ )  $\delta$  12.74 (br s, 1 H), 8.32 (dd,  $J = 6.0$  Hz, 8.7 Hz, 2

H), 7.55–7.66 (m, 2 H), 7.48 (d,  $J = 8.0$  Hz, 1 H), 7.24 (dd,  $J = 8.9$  Hz, 8.9 Hz, 2 H), 7.14–7.19 (m, 1 H), 4.75–4.90 (m, 1 H), 3.99–4.10 (m, 2 H), 3.45–3.77 (m, 2 H), 2.69–2.84 (m, 2 H), 2.52–2.63 (m, 2 H), 2.25–2.41 (m, 2 H), 2.09–2.19 (m, 2 H), 1.54–1.79 (m, 8 H), 1.11 (d,  $J = 6.7$  Hz, 6 H), 1.03 (s, 6 H). HRMS ( $m/z$ ):  $[MH^+]$  calcd for  $C_{32}H_{43}FN_5O_3$ , 564.3344; found, 564.3346.

**(E)-4-Fluoro-N-(6-(((2-hydroxy-2-methylpropyl)amino)methyl)-1-((1*s*,4*s*)-4-(isopropylcarbamoyl)cyclohexyl)-1*H*-benzo[d]imidazol-2(3*H*)-ylidene)benzamide (39).** General procedure B, with 1-amino-2-methylpropan-2-ol (Tyger Scientific, 197 mg, 2.21 mmol), was used to produce 39 (24 mg, 17.1% yield) as a white solid.  $^1H$  NMR (400 MHz, DMSO- $d_6$ )  $\delta$  12.75 (br s, 1 H), 8.32 (dd,  $J = 5.8$  Hz, 8.6 Hz, 2 H), 7.60–7.70 (m, 2 H), 7.49 (d,  $J = 8.2$  Hz, 1 H), 7.19–7.28 (m, 3 H), 4.75–4.88 (m, 1 H), 2.72–2.87 (m, 2 H), 3.99–4.10 (m, 1 H), 3.79–3.93 (m, 2 H), 2.52–2.57 (m, 1 H), 2.40–2.48 (m, 1 H), 2.09–2.17 (m, 2 H), 1.56–1.79 (m, 4 H), 1.23–1.28 (m, 2 H), 1.06–1.15 (m, 12 H). HRMS ( $m/z$ ):  $[MH^+]$  calcd for  $C_{29}H_{39}FN_5O_3$ , 524.3031; found, 524.3032.

**(E)-4-Fluoro-N-(6-(((3-(2-hydroxypropan-2-yl)azetidin-1-yl)methyl)-1-((1*s*,4*s*)-4-(isopropylcarbamoyl)cyclohexyl)-1*H*-benzo[d]imidazol-2(3*H*)-ylidene)benzamide (40).** General Procedure B, with 2-(azetidin-3-yl)propan-2-ol hydrochloride<sup>25</sup> (101 mg, 0.66 mmol) and DBU (0.10 mL, 0.66 mmol), was used to produce 40 (26 mg, 21.4% yield) as a white solid.  $^1H$  NMR (400 MHz, DMSO- $d_6$ )  $\delta$  12.77 (br s, 1 H), 8.27–8.36 (m, 2 H), 7.55–7.70 (m, 2 H), 7.50 (d,  $J = 5.9$  Hz, 1 H), 7.24 (dd,  $J = 8.9$  Hz, 8.9 Hz, 2 H), 7.12–7.20 (m, 1 H), 4.76–4.89 (m, 1 H), 4.01–4.11 (m, 1 H), 3.29 (s, 2 H), 2.70–2.85 (m, 2 H), 2.52–2.57 (m, 1 H), 2.09–2.19 (m, 2 H), 1.67–1.79 (m, 2 H), 1.57–1.67 (m, 2 H), 1.21–1.30 (m, 2 H), 1.11 (d,  $J = 6.6$  Hz, 6 H), 1.02 (s, 6 H). HRMS ( $m/z$ ):  $[MH^+]$  calcd for  $C_{31}H_{41}FN_5O_3$ , 550.3188; found, 550.3192.

**2-(1-(3-Fluoro-4-nitrobenzyl)piperidin-4-yl)propan-2-ol (42).** To a solution of 3-fluoro-4-nitrobenzaldehyde (Bionet Research, 5.50 g, 32.5 mmol) in DCM (100 mL) was added acetic acid (0.17 mL). The reaction was cooled in an ice–water bath to 5 °C, and then 23 (4.66 g, 32.5 mmol) was added, followed by sodium triacetoxyborohydride (7.10 g, 33.5 mmol) and additional DCM (50 mL). The reaction was stirred at 5 °C for 45 min, allowed to warm to ambient temperature, and stirred at ambient temperature for 1 h. The reaction mixture was concentrated, and the residue was diluted with ethyl acetate and washed with saturated aqueous sodium bicarbonate and brine. The organic phase was concentrated, adsorbed onto a silica-gel loading column, and purified by chromatography, eluting with 50–100% ethyl acetate in hexanes, to afford 42 (8.48 g, 88% yield) as a yellow oil.  $^1H$  NMR (400 MHz,  $CDCl_3$ )  $\delta$  8.02 (t,  $J = 8.0$  Hz, 1 H), 7.34 (d,  $J = 8.1$  Hz, 1 H), 7.27 (br s, 1 H), 3.55 (br s, 2 H), 2.87–2.98 (m, 2 H), 1.95–2.07 (m, 2 H), 1.53–1.87 (m, 2 H), 1.37–1.50 (m, 2 H), 1.29–1.35 (m, 1 H), 1.20 (s, 6 H). LC/MS ( $ESI^+$ )  $m/z = 297.2$  (M + H).

**(1*s*,4*s*)-4-(((5-(((4-(2-Hydroxypropan-2-yl)piperidin-1-yl)methyl)-2-nitrophenyl)amino)-*N*-isopropylcyclohexanecarboxamide (43).** To a solution of 42 (8.48 g, 28.6 mmol) in acetonitrile (50 mL) was added 19 (7.10 g, 32.2 mmol), followed by *N,N*-diisopropylethylamine (14.9 mL, 86 mmol). The reaction was stirred for 15 min at ambient temperature and then at 80 °C for 24 h. After cooling to ambient temperature, the reaction mixture was concentrated in vacuo, and the residue was partitioned between ethyl acetate and aqueous potassium carbonate. The aqueous layer was extracted with ethyl acetate three times; the combined organic phases were washed with brine and concentrated. The crude product was adsorbed onto a silica gel pad and eluted with ethyl acetate, followed by 90:10:1 DCM:methanol:ammonium hydroxide when the product began to elute. The product fractions were combined and concentrated; the residue was recrystallized from hot toluene/hexanes to afford 43 (9.62 g, 73% yield).  $^1H$  NMR (400 MHz, DMSO- $d_6$ )  $\delta$  8.28 (d,  $J = 7.5$  Hz, 1 H), 8.03 (d,  $J = 8.9$  Hz, 1 H), 7.54 (d,  $J = 7.7$  Hz, 1 H), 6.97 (s, 1 H), 6.65 (dd,  $J = 1.5$  Hz, 8.9 Hz, 1 H), 4.01 (s, 1 H), 3.88–3.95 (m, 1 H), 3.77–3.87 (m, 1 H), 3.43 (s, 2 H), 2.70–2.98 (m, 2 H), 2.17–2.25 (m, 1 H), 1.79–1.92 (m, 4 H), 1.58–1.74 (m, 8

H), 1.10–1.30 (m, 3 H), 1.03 (d,  $J = 6.5$  Hz, 6 H), 1.03 (s, 6 H). LC/MS ( $ESI^+$ )  $m/z = 461.2$  (M + H).

**(1*s*,4*s*)-4-((2-Amino-5-(((4-(2-hydroxypropan-2-yl)piperidin-1-yl)methyl)phenyl)amino)-*N*-isopropylcyclohexanecarboxamide (44).** To a slurry of 5% palladium on carbon (1.42 g, 0.667 mmol) in water (10 mL), under an argon atmosphere, was added ethanol (100 mL), followed by 43 (9.62 g, 20.9 mmol). The reaction was cooled in an ice–water bath, and ammonium formate (13.2 g, 209 mmol), and ethanol (20 mL) were added. The reaction was stirred at 5 °C for 135 min. The reaction was filtered through a Celite pad, and the filter cake was rinsed with ethanol and DCM. The combined filtrates were concentrated and partitioned between DCM and water. The aqueous layer was extracted twice with 1-butanol; the combined organic layers were washed with brine and concentrated. The crude product was adsorbed onto a silica gel pad and eluted with ethyl acetate, followed by 90:10:1 DCM:methanol:ammonium hydroxide when the product began to elute. The product-containing filtrate was concentrated; the resulting foam was recrystallized from toluene/hexanes to afford 44 (8.98 g, 100% yield) as a red solid.  $^1H$  NMR (400 MHz,  $CDCl_3$ )  $\delta$  6.68 (d,  $J = 1.4$  Hz, 1 H), 6.66 (d,  $J = 7.8$  Hz, 1 H), 6.58 (dd,  $J = 1.7$  Hz, 7.8 Hz, 1 H), 5.28 (d,  $J = 7.7$  Hz, 1 H), 4.05–4.18 (m, 1 H), 3.57–3.63 (m, 1 H), 3.54 (s, 2 H), 2.97–3.21 (m, 2 H), 2.13–2.21 (m, 1 H), 1.98–2.07 (m, 2 H), 1.82–1.92 (m, 3 H), 1.66–1.77 (m, 6 H), 1.45–1.56 (m, 2 H), 1.26–1.35 (m, 1 H), 1.18 (s, 6 H), 1.16 (d,  $J = 6.6$  Hz, 6 H).

**3,5-Difluorobenzoyl Isothiocyanate (45).** To a solution of potassium thiocyanate (5.65 mL, 111 mmol) in acetonitrile (65 mL) was added 3,5-difluorobenzoyl chloride (16.3 g, 92 mmol) dropwise via syringe, and the reaction was stirred for 2 h at 50 °C. After the reaction was complete, the reaction mixture was cooled to ambient temperature and the precipitated solids were removed by filtration. The filtrate was concentrated, and the residue was triturated with benzene. The precipitated solids were again removed by filtration, and the filtrate was concentrated. The residue was triturated with 3:2 benzene/hexanes, and the precipitated solids were again removed by filtration. The filtrate was concentrated in vacuo to generate 45 (10.9 g, 59% yield) as a light-orange liquid.  $^1H$  NMR (400 MHz,  $CDCl_3$ )  $\delta$  7.56–7.62 (m, 2 H), 7.12 (tt,  $J = 2.4$  Hz, 8.3 Hz, 1 H).

**(1*s*,4*s*)-4-(2-Amino-6-(((4-(2-hydroxypropan-2-yl)piperidin-1-yl)methyl)-1*H*-benzo[d]imidazol-1-yl)-*N*-isopropylcyclohexanecarboxamide (46).** Step 1: To a solution of 44 (1.86 g, 4.32 mmol) in 1,4-dioxane (22 mL) was added acetyl isothiocyanate (0.379 mL, 4.32 mmol), and the reaction was stirred at 100 °C for 5 min. After the reaction had cooled to ambient temperature, 1-(3-dimethylaminopropyl)-3-ethylcarbodiimide hydrochloride (2.48 g, 13.0 mmol) and *N,N*-diisopropylethylamine (2.72 mL, 15.6 mmol) were added, and the reaction was stirred at 60 °C for 1 h. The reaction mixture was then concentrated onto silica gel and purified by column chromatography, eluting with 90:10:1 DCM:methanol:ammonium hydroxide. The product fractions were combined and concentrated to produce (1*s*,4*s*)-4-(2-acetamido-6-(((4-(2-hydroxypropan-2-yl)piperidin-1-yl)methyl)-1*H*-benzo[d]imidazol-1-yl)-*N*-isopropylcyclohexanecarboxamide as an orange solid. LC/MS ( $ESI^+$ )  $m/z = 498.2$  (M + H).

Step 2: A solution of (1*s*,4*s*)-4-(2-acetamido-6-(((4-(2-hydroxypropan-2-yl)piperidin-1-yl)methyl)-1*H*-benzo[d]imidazol-1-yl)-*N*-isopropylcyclohexanecarboxamide (2.16 g, 4.34 mmol) in 2 N aqueous HCl (33 mL) was stirred at 50 °C for 24 h. After concentrating the reaction mixture in vacuo, the crude product was adsorbed onto a silica gel loading column and purified by column chromatography, eluting with a gradient of 0–100% [9:1 DCM:methanol with 1% ammonium hydroxide] in DCM. The product fractions were combined and concentrated to produce 46 (1.63 g, 82% yield over two steps).  $^1H$  NMR (400 MHz, DMSO- $d_6$ )  $\delta$  7.60 (d,  $J = 7.6$  Hz, 1 H), 7.20 (s, 1 H), 7.02 (d,  $J = 8.0$  Hz, 1 H), 6.84 (d,  $J = 8.0$  Hz, 1 H), 6.19 (s, 2 H), 4.19 (br s, 1 H), 3.93–4.03 (m, 2 H), 3.40 (s, 2 H), 2.75–2.99 (m, 2 H), 2.41–2.47 (m, 2 H), 1.95–2.25 (m, 2 H), 1.78 (br s, 2 H), 1.50–1.65 (m, 6 H), 1.16–1.28 (m, 4 H), 1.12 (d,  $J = 6.5$  Hz, 6 H), 1.01 (s, 6 H). LC/MS ( $ESI^+$ )  $m/z = 456.2$  (M + H).

**Preparation of 47–48 and 50–59. General Procedure C.** To a solution of **46** (100 mg, 0.219 mmol), 1-(3-dimethylaminopropyl)-3-ethylcarbodiimide hydrochloride (0.063 g, 0.329 mmol), *N*-hydroxybenzotriazole (0.034 g, 0.219 mmol), and *N,N*-diisopropylethylamine (0.153 mL, 0.878 mmol) in DMF (0.439 mL) was added a benzoic acid (0.219 mmol). The reaction was stirred at 50 °C for 2 h and then stirred at ambient temperature overnight. The reaction mixture was diluted with ethyl acetate and washed with water and brine; the organic layer was dried over sodium sulfate, filtered, and concentrated. The crude product was purified via reverse-phase preparative HPLC to provide the desired product.

**(*E*)-*N*-(6-((4-(2-Hydroxypropan-2-yl)piperidin-1-yl)methyl)-1-((1*s*,4*s*)-4-(isopropylcarbamoyl)cyclohexyl)-1*H*-benzo[d]imidazol-2(3*H*)-ylidene)benzamide (47).** The title compound was prepared by general procedure C using benzoic acid. The crude product was purified using a gradient of 20–80% [0.1% TFA in acetonitrile] in [0.1% TFA in water] to produce **47** (27 mg, 22.3% yield). <sup>1</sup>H NMR (400 MHz, DMSO-*d*<sub>6</sub>) δ 12.75 (br s, 1 H), 8.26 (d, *J* = 7.2 Hz, 2 H), 7.63 (d, *J* = 7.6 Hz, 1 H), 7.56 (s, 1 H), 7.43–7.53 (m, 4 H), 7.15 (d, *J* = 8.1 Hz, 1 H), 4.79–4.93 (m, 1 H), 4.03–4.12 (m, 1 H), 4.01 (s, 1 H), 3.51 (s, 2 H), 2.82–2.96 (m, 2 H), 2.65–2.78 (m, 2 H), 2.51–2.56 (m, 1 H), 2.11–2.21 (m, 2 H), 1.78–1.93 (m, 2 H), 1.55–1.78 (m, 6 H), 1.20–1.32 (m, 2 H), 1.13–1.18 (m, 1 H), 1.11 (d, *J* = 6.6 Hz, 6 H), 1.02 (s, 6 H). HRMS (*m/z*): [MH<sup>+</sup>] calcd for C<sub>33</sub>H<sub>46</sub>N<sub>5</sub>O<sub>3</sub>, 560.3595; found, 560.3598.

**(*E*)-3-Fluoro-*N*-(6-((4-(2-hydroxypropan-2-yl)piperidin-1-yl)methyl)-1-((1*s*,4*s*)-4-(isopropylcarbamoyl)cyclohexyl)-1*H*-benzo[d]imidazol-2(3*H*)-ylidene)benzamide (48).** The title compound was prepared by general procedure C using 3-fluorobenzoic acid. The crude product was purified using a gradient of 20–80% [0.1% TFA in acetonitrile] in [0.1% TFA in water] to produce **48** (33 mg, 39.5% yield). <sup>1</sup>H NMR (400 MHz, DMSO-*d*<sub>6</sub>) δ 12.80 (br s, 1 H), 8.11 (d, *J* = 7.8 Hz, 1 H), 7.94 (d, *J* = 9.9 Hz, 1 H), 7.43–7.69 (m, 4 H), 7.29–7.39 (m, 1 H), 7.11–7.23 (m, 1 H), 4.80–4.92 (m, 1 H), 3.94–4.13 (m, 2 H), 3.44–3.58 (m, 2 H), 2.81–2.96 (m, 2 H), 2.64–2.80 (m, 2 H), 2.51–2.56 (m, 1 H), 2.09–2.21 (m, 2 H), 1.54–1.92 (m, 8 H), 1.20–1.37 (m, 2 H), 1.13–1.19 (m, 1 H), 1.10 (d, *J* = 6.6 Hz, 6 H), 1.02 (s, 6 H). HRMS (*m/z*): [MH<sup>+</sup>] calcd for C<sub>33</sub>H<sub>45</sub>FN<sub>5</sub>O<sub>3</sub>, 578.3501; found, 578.3500.

**(*E*)-3,5-Difluoro-*N*-(6-((4-(2-hydroxypropan-2-yl)piperidin-1-yl)methyl)-1-((1*s*,4*s*)-4-(isopropylcarbamoyl)cyclohexyl)-1*H*-benzo[d]imidazol-2(3*H*)-ylidene)benzamide (49).** To a solution of **44** (8.98 g, 20.9 mmol) in THF (80 mL) at 0 °C was added a solution of **45** (4.57 g, 22.9 mmol) in THF. The reaction was stirred at 0 °C for 30 min and then warmed to 20 °C and stirred for 1.5 h to form the thiourea intermediate.

To the reaction mixture were added *N,N*-diisopropylethylamine (4.37 mL, 25.02 mmol) and 1-(3-dimethylaminopropyl)-3-ethylcarbodiimide hydrochloride (4.80 g, 25.02 mmol), and the reaction was stirred at 60 °C for 1 h. The reaction mixture was diluted with ethyl acetate, washed with water and brine, and concentrated. The crude product was adsorbed onto a silica gel loading column and purified by column chromatography, eluting with 1:1 ethyl acetate/hexanes, followed by 5–10% [9:1 DCM/methanol with 1% ammonium hydroxide] in DCM. The product fractions were combined and concentrated; the residue was recrystallized from acetonitrile to produce **49** (8.95 g, 72% yield) as an off-white crystalline solid. <sup>1</sup>H NMR (400 MHz, DMSO-*d*<sub>6</sub>) δ 12.81 (s, 1 H), 7.85 (dd, *J* = 2.3 Hz, 8.4 Hz, 2 H), 7.56–7.64 (m, 2 H), 7.50 (d, *J* = 8.2 Hz, 1 H), 7.38 (tt, *J* = 9.0 Hz, 2.4 Hz, 1 H), 7.18 (dd, *J* = 8.2 Hz, 8.2 Hz, 1 H), 4.78–4.90 (m, 1 H), 4.00–4.11 (m, 1 H), 3.99 (s, 1 H), 3.50 (s, 2 H), 2.85–2.92 (m, 2 H), 2.63–2.82 (m, 2 H), 2.51–2.56 (m, 1 H), 2.06–2.19 (m, 2 H), 1.69–1.91 (m, 4 H), 1.56–1.69 (m, 4 H), 1.18–1.35 (m, 2 H), 1.12–1.18 (m, 1 H), 1.09 (d, *J* = 3.6 Hz, 6 H), 1.02 (s, 6 H). HRMS (*m/z*): [MH<sup>+</sup>] calcd for C<sub>33</sub>H<sub>44</sub>F<sub>2</sub>N<sub>5</sub>O<sub>3</sub>, 596.3407; found, 596.3409.

**(*E*)-*N*-(6-((4-(2-Hydroxypropan-2-yl)piperidin-1-yl)methyl)-1-((1*s*,4*s*)-4-(isopropylcarbamoyl)cyclohexyl)-1*H*-benzo[d]imidazol-2(3*H*)-ylidene)isonicotinamide (50).** The title compound was prepared by general procedure C using isonicotinic acid. The crude product was purified using a gradient of 15–75% [0.1%

TFA in acetonitrile] in [0.1% TFA in water] to produce **50** (27 mg, 21.3% yield). <sup>1</sup>H NMR (400 MHz, DMSO-*d*<sub>6</sub>) δ 12.83 (s, 1 H), 8.70 (dd, *J* = 1.5 Hz, 4.5 Hz, 2H), 8.11 (dd, *J* = 1.5 Hz, 4.5 Hz, 2 H), 7.63 (d, *J* = 7.6 Hz, 1 H), 7.58 (s, 1 H), 7.50 (d, *J* = 8.1 Hz, 1 H), 7.18 (d, *J* = 8.1 Hz, 1 H), 4.80–4.91 (m, 1 H), 4.02–4.11 (m, 1 H), 4.00 (s, 1 H), 3.50 (s, 2 H), 2.85–2.93 (m, 2 H), 2.69–2.81 (m, 2 H), 2.52–2.56 (m, 1 H), 2.12–2.20 (m, 2 H), 1.79–1.88 (m, 2 H), 1.68–1.79 (m, 2 H), 1.58–1.68 (m, 4 H), 1.20–1.31 (m, 2 H), 1.12–1.18 (m, 1 H), 1.10 (d, *J* = 6.5 Hz, 6 H), 1.02 (s, 6 H). HRMS (*m/z*): [MH<sup>+</sup>] calcd for C<sub>32</sub>H<sub>45</sub>N<sub>6</sub>O<sub>3</sub>, 561.3548; found, 561.3548.

**(*E*)-4-Cyano-*N*-(6-((4-(2-Hydroxypropan-2-yl)piperidin-1-yl)methyl)-1-((1*s*,4*s*)-4-(isopropylcarbamoyl)cyclohexyl)-1*H*-benzo[d]imidazol-2(3*H*)-ylidene)benzamide (51).** The title compound was prepared by general procedure C using 4-cyanobenzoic acid. The crude product was purified using a gradient of 20–80% [0.1% TFA in acetonitrile] in [0.1% TFA in water] to produce **51** (32 mg, 20.5% yield). <sup>1</sup>H NMR (400 MHz, DMSO-*d*<sub>6</sub>) δ 12.83 (br s, 1 H), 8.41 (d, *J* = 8.4 Hz, 2 H), 7.91 (d, *J* = 8.4 Hz, 2 H), 7.64 (d, *J* = 7.6 Hz, 1 H), 7.58 (s, 1 H), 7.50 (d, *J* = 8.1 Hz, 1 H), 7.18 (d, *J* = 8.2 Hz, 1 H), 4.81–4.92 (m, 1 H), 4.01–4.09 (m, 1 H), 4.00 (s, 1 H), 3.50 (s, 2 H), 2.83–2.93 (m, 2 H), 2.66–2.80 (m, 2 H), 2.52–2.56 (m, 1 H), 2.10–2.19 (m, 2 H), 1.79–1.89 (m, 2 H), 1.68–1.79 (m, 2 H), 1.58–1.67 (m, 4 H), 1.18–1.31 (m, 2 H), 1.13–1.17 (m, 1 H), 1.11 (d, *J* = 6.5 Hz, 6 H), 1.02 (s, 6 H). HRMS (*m/z*): [MH<sup>+</sup>] calcd for C<sub>34</sub>H<sub>45</sub>N<sub>6</sub>O<sub>3</sub>, 585.3548; found, 585.3549.

**(*E*)-*N*-(6-((4-(2-Hydroxypropan-2-yl)piperidin-1-yl)methyl)-1-((1*s*,4*s*)-4-(isopropylcarbamoyl)cyclohexyl)-1*H*-benzo[d]imidazol-2(3*H*)-ylidene)nicotinamide (52).** The title compound was prepared by general procedure C using nicotinic acid. The crude product was purified using a gradient of 15–75% [0.1% TFA in acetonitrile] in [0.1% TFA in water] to produce **52** (27 mg, 23.2% yield). <sup>1</sup>H NMR (400 MHz, DMSO-*d*<sub>6</sub>) δ 12.79 (s, 1 H), 9.36 (d, *J* = 1.4 Hz, 1 H), 8.69 (dd, *J* = 1.7 Hz, 4.7 Hz, 1 H), 8.56 (d, *J* = 7.8 Hz, 1 H), 7.63 (d, *J* = 7.6 Hz, 1 H), 7.58 (s, 1 H), 7.46–7.53 (m, 2 H), 7.18 (d, *J* = 8.2 Hz, 1 H), 4.85–4.94 (m, 1 H), 4.02–4.11 (m, 1 H), 4.01 (s, 1 H), 3.50 (s, 2 H), 2.83–2.93 (m, 2 H), 2.66–2.77 (m, 2 H), 2.51–2.56 (m, 1 H), 2.12–2.19 (m, 2 H), 1.80–1.88 (m, 2 H), 1.69–1.80 (m, 2 H), 1.58–1.69 (m, 4 H), 1.20–1.32 (m, 2 H), 1.13–1.17 (m, 1 H), 1.11 (d, *J* = 6.5 Hz, 6 H), 1.02 (s, 6 H). HRMS (*m/z*): [MH<sup>+</sup>] calcd for C<sub>32</sub>H<sub>45</sub>N<sub>6</sub>O<sub>3</sub>, 561.3548; found, 561.3552.

**(*E*)-3,4-Difluoro-*N*-(6-((4-(2-hydroxypropan-2-yl)piperidin-1-yl)methyl)-1-((1*s*,4*s*)-4-(isopropylcarbamoyl)cyclohexyl)-1*H*-benzo[d]imidazol-2(3*H*)-ylidene)benzamide (53).** The title compound was prepared by general procedure C using 3,4-difluorobenzoic acid. The crude product was purified using a gradient of 30–90% [0.1% TFA in acetonitrile] in [0.1% TFA in water] to produce **53** (35 mg, 16.4% yield). <sup>1</sup>H NMR (400 MHz, DMSO-*d*<sub>6</sub>) δ 12.77 (s, 1 H), 8.15–8.22 (m, 1 H), 8.09–8.15 (m, 1 H), 7.63 (d, *J* = 7.7 Hz, 1 H), 7.56 (s, 1 H), 7.44–7.52 (m, 2 H), 7.16 (d, *J* = 8.3 Hz, 1 H), 4.77–4.88 (m, 1 H), 4.01–4.10 (m, 1 H), 4.00 (s, 1 H), 3.49 (s, 2 H), 2.84–2.93 (m, 2 H), 2.68–2.80 (m, 2 H), 2.51–2.56 (m, 1 H), 2.07–2.18 (m, 2 H), 1.79–1.88 (m, 2 H), 1.68–1.79 (m, 2 H), 1.55–1.68 (m, 4 H), 1.20–1.32 (m, 2 H), 1.12–1.17 (m, 1 H), 1.10 (d, *J* = 6.6 Hz, 6 H), 1.02 (s, 6 H). HRMS (*m/z*): [MH<sup>+</sup>] calcd for C<sub>33</sub>H<sub>44</sub>F<sub>2</sub>N<sub>5</sub>O<sub>3</sub>, 596.3407; found, 596.3406.

**(*E*)-3-Cyano-5-fluoro-*N*-(6-((4-(2-hydroxypropan-2-yl)piperidin-1-yl)methyl)-1-((1*s*,4*s*)-4-(isopropylcarbamoyl)cyclohexyl)-1*H*-benzo[d]imidazol-2(3*H*)-ylidene)benzamide (54).** The title compound was prepared by general procedure C using 3-cyano-5-fluorobenzoic acid. The crude product was purified using a gradient of 30–90% [0.1% TFA in acetonitrile] in [0.1% TFA in water] to produce **54** (36 mg, 17.6% yield). <sup>1</sup>H NMR (400 MHz, DMSO-*d*<sub>6</sub>) δ 12.87 (br s, 1 H), 8.43 (s, 1 H), 8.32 (d, *J* = 1.0 Hz, 1 H), 7.96–8.03 (m, 1 H), 7.58–7.65 (m, 2 H), 7.52 (d, *J* = 8.1 Hz, 1 H), 7.19 (d, *J* = 8.2 Hz, 1 H), 4.78–4.90 (m, 1 H), 4.02–4.13 (m, 1 H), 4.00 (s, 1 H), 3.50 (s, 2 H), 2.85–2.92 (m, 2 H), 2.72–2.84 (m, 2 H), 2.52–2.57 (m, 1 H), 2.06–2.15 (m, 2 H), 1.68–1.90 (m, 4 H), 1.58–1.67 (m, 4 H), 1.19–1.31 (m, 2 H), 1.11–1.18 (m, 1 H), 1.08 (d, *J* = 6.5 Hz, 6 H), 1.02 (s, 6 H). HRMS (*m/z*): [MH<sup>+</sup>] calcd for C<sub>34</sub>H<sub>44</sub>FN<sub>6</sub>O<sub>3</sub>, 603.3453; found, 603.3452.

(*E*)-3-Cyano-*N*-(6-((4-(2-hydroxypropan-2-yl)piperidin-1-yl)methyl)-1-((1*S*,4*S*)-4-(isopropylcarbamoyl)cyclohexyl)-1*H*-benzo[d]imidazol-2(3*H*)-ylidene)benzamide (55). The title compound was prepared by general procedure C using 3-cyanobenzoic acid. The crude product was purified using a gradient of 20–80% [0.1% TFA in acetonitrile] in [0.1% TFA in water] to produce 55 (32 mg, 20.2% yield). <sup>1</sup>H NMR (400 MHz, DMSO-*d*<sub>6</sub>) δ 12.83 (br s, 1 H), 8.60 (d, *J* = 7.9 Hz, 1 H), 8.56 (s, 1 H), 7.98 (dd, *J* = 1.3 Hz, 7.7 Hz, 1 H), 7.68 (dd, *J* = 7.7 Hz, 7.7 Hz, 1 H), 7.63 (d, *J* = 7.6 Hz, 1 H), 7.58 (s, 1 H), 7.51 (d, *J* = 8.2 Hz, 1 H), 7.17 (d, *J* = 8.1 Hz, 1 H), 4.80–4.91 (m, 1 H), 4.03–4.13 (m, 1 H), 4.00 (s, 1 H), 3.50 (s, 2 H), 2.83–2.93 (m, 2 H), 2.69–2.83 (m, 2 H), 2.51–2.56 (m, 1 H), 2.08–2.19 (m, 2 H), 1.69–1.90 (m, 4 H), 1.55–1.69 (m, 4 H), 1.18–1.31 (m, 2 H), 1.12–1.18 (m, 1 H), 1.10 (d, *J* = 6.5 Hz, 6 H), 1.01 (s, 6 H). HRMS (*m/z*): [MH<sup>+</sup>] calcd for C<sub>34</sub>H<sub>45</sub>N<sub>6</sub>O<sub>3</sub>, 585.3548; found, 585.3548.

(*E*)-3-Chloro-5-fluoro-*N*-(6-((4-(2-hydroxypropan-2-yl)piperidin-1-yl)methyl)-1-((1*S*,4*S*)-4-(isopropylcarbamoyl)cyclohexyl)-1*H*-benzo[d]imidazol-2(3*H*)-ylidene)benzamide (56). The title compound was prepared by general procedure C using 3-chloro-5-fluorobenzoic acid. The crude product was purified using a gradient of 30–90% [0.1% TFA in acetonitrile] in [0.1% TFA in water] to produce 56 (38 mg, 21.4% yield). <sup>1</sup>H NMR (400 MHz, DMSO-*d*<sub>6</sub>) δ 12.82 (br s, 1 H), 7.96–8.05 (m, 2 H), 7.54–7.66 (m, 3 H), 7.51 (d, *J* = 8.1 Hz, 1 H), 7.18 (d, *J* = 8.1 Hz, 1 H), 4.80–4.91 (m, 1 H), 4.01–4.10 (m, 1 H), 4.00 (s, 1 H), 3.50 (s, 2 H), 2.84–2.92 (m, 2 H), 2.64–2.79 (m, 2 H), 2.51–2.56 (m, 1 H), 2.05–2.19 (m, 2 H), 1.79–1.89 (m, 2 H), 1.67–1.79 (m, 2 H), 1.59–1.67 (m, 4 H), 1.12–1.31 (m, 3 H), 1.10 (d, *J* = 6.5 Hz, 6 H), 1.02 (s, 6 H). HRMS (*m/z*): [MH<sup>+</sup>] calcd for C<sub>33</sub>H<sub>44</sub>ClFN<sub>5</sub>O<sub>3</sub>, 612.3111; found, 612.3116.

(*E*)-3-Chloro-*N*-(6-((4-(2-hydroxypropan-2-yl)piperidin-1-yl)methyl)-1-((1*S*,4*S*)-4-(isopropylcarbamoyl)cyclohexyl)-1*H*-benzo[d]imidazol-2(3*H*)-ylidene)benzamide (57). The title compound was prepared by general procedure C using 3-chlorobenzoic acid. The crude product was purified using a gradient of 30–90% [0.1% TFA in acetonitrile] in [0.1% TFA in water] to produce 57 (34 mg, 21.4% yield). <sup>1</sup>H NMR (400 MHz, DMSO-*d*<sub>6</sub>) δ 12.82 (br s, 1 H), 7.96–8.05 (m, 2 H), 7.54–7.66 (m, 3 H), 7.51 (d, *J* = 8.1 Hz, 1 H), 7.18 (d, *J* = 8.1 Hz, 1 H), 4.80–4.91 (m, 1 H), 4.01–4.10 (m, 1 H), 4.00 (s, 1 H), 3.50 (s, 2 H), 2.84–2.92 (m, 2 H), 2.51–2.56 (m, 1 H), 2.05–2.19 (m, 2 H), 1.79–1.89 (m, 2 H), 1.59–1.67 (m, 4 H), 1.18–1.31 (m, 2 H), 1.14–1.17 (m, 1 H), 1.10 (d, *J* = 6.5 Hz, 6 H), 1.02 (s, 6 H). HRMS (*m/z*): [MH<sup>+</sup>] calcd for C<sub>33</sub>H<sub>45</sub>ClN<sub>5</sub>O<sub>3</sub>, 594.3205; found, 594.3204.

(*E*)-3-Chloro-4-fluoro-*N*-(6-((4-(2-hydroxypropan-2-yl)piperidin-1-yl)methyl)-1-((1*S*,4*S*)-4-(isopropylcarbamoyl)cyclohexyl)-1*H*-benzo[d]imidazol-2(3*H*)-ylidene)benzamide (58). The title compound was prepared by general procedure C using 3-chloro-4-fluorobenzoic acid. The crude product was purified using a gradient of 30–90% [0.1% TFA in acetonitrile] in [0.1% TFA in water] to produce 58 (38 mg, 21.4% yield). <sup>1</sup>H NMR (400 MHz, DMSO-*d*<sub>6</sub>) δ 12.77 (br s, 1 H), 8.27–8.34 (m, 2 H), 7.63 (d, *J* = 7.6 Hz, 1 H), 7.57 (s, 1 H), 7.43–7.54 (m, 2 H), 7.16 (d, *J* = 8.2 Hz, 1 H), 4.80–4.90 (m, 1 H), 4.02–4.11 (m, 1 H), 4.00 (s, 1 H), 3.49 (s, 2 H), 2.84–2.92 (m, 2 H), 2.66–2.79 (m, 2 H), 2.51–2.57 (m, 1 H), 2.09–2.18 (m, 2 H), 1.78–1.88 (m, 2 H), 1.67–1.78 (m, 2 H), 1.55–1.67 (m, 4 H), 1.20–1.30 (m, 2 H), 1.12–1.17 (m, 1 H), 1.11 (d, *J* = 6.5 Hz, 6 H), 1.01 (s, 6 H). HRMS (*m/z*): [MH<sup>+</sup>] calcd for C<sub>33</sub>H<sub>44</sub>ClFN<sub>5</sub>O<sub>3</sub>, 612.3111; found, 612.3111.

(*E*)-4-Cyano-3-fluoro-*N*-(6-((4-(2-hydroxypropan-2-yl)piperidin-1-yl)methyl)-1-((1*S*,4*S*)-4-(isopropylcarbamoyl)cyclohexyl)-1*H*-benzo[d]imidazol-2(3*H*)-ylidene)benzamide (59). The title compound was prepared by general procedure C using 4-cyano-3-fluorobenzoic acid. The crude product was purified using a gradient of 30–90% [0.1% TFA in acetonitrile] in [0.1% TFA in water] to produce 59 (36 mg, 21.5% yield). <sup>1</sup>H NMR (400 MHz, DMSO-*d*<sub>6</sub>) δ 12.87 (br s, 1 H), 8.20–8.27 (m, 2 H), 7.96–8.02 (m, 1 H), 7.57–7.67 (m, 2 H), 7.52 (d, *J* = 8.2 Hz, 1 H), 7.19 (d, *J* = 8.1 Hz, 1 H), 4.79–4.90 (m, 1 H), 4.01–4.10 (m, 1 H), 4.00 (s, 1 H), 3.50 (s, 2 H), 2.83–2.93 (m, 2 H), 2.70–2.82 (m, 2 H), 2.51–2.56 (m, 1 H), 2.08–2.16 (m, 2 H), 1.69–1.89 (m, 4 H), 1.59–1.67 (m, 4 H), 1.19–1.31 (m, 2 H), 1.12–1.18 (m, 1 H), 1.10 (d, *J* = 6.6 Hz, 6 H), 1.02 (s,

6 H). HRMS (*m/z*): [MH<sup>+</sup>] calcd for C<sub>34</sub>H<sub>44</sub>FN<sub>6</sub>O<sub>3</sub>, 603.3453; found, 603.3450.

## ■ ASSOCIATED CONTENT

### Supporting Information

IC<sub>50</sub> data from which the selectivity ratios are derived for the off-target kinases, together with protocols for in vitro selectivity assays, xenograft study, and X-ray crystallography. This material is available free of charge via the Internet at <http://pubs.acs.org>.

## ■ AUTHOR INFORMATION

### Corresponding Author

\*Phone: 617-444-5232. Fax: 617-577-9511. E-mail: richard.lewis@amgen.com.

### Notes

The authors declare the following competing financial interest(s): The authors are employees of Amgen Inc.

## ■ ACKNOWLEDGMENTS

Kavita Shah and Roman Shimanovich are thanked for their assistance with formulation of compounds for in vivo studies. Jingzhou Liu, Loren Berry, Samer A. Al-Assaad, and James Mann are thanked for their assistance with in vitro screening assays. Alan Cheng is thanked for stimulating discussions and in-silico modeling assistance. Keith Wilcoxon of TESARO is thanked for helpful discussions.

## ■ ABBREVIATIONS USED

ALK, anaplastic lymphoma kinase; ALCL, anaplastic large-cell lymphoma; ATP, adenosine triphosphate; c-Met, hepatocyte growth factor receptor tyrosine kinase; DCC, *N,N*-dicyclohexylcarbodiimide; DCE, dichloroethane; DCM, dichloromethane; DFG, Asp-Phe-Gly sequence in ATP binding site; DIPEA, diisopropylethylamine; EDCI, *N*-(3-dimethylaminopropyl)-*N*'-ethylcarbodiimide hydrochloride; EML4-ALK, echinoderm microtubule-associated protein-like 4-ALK fusion protein; FRET, fluorescence resonance energy transfer; HATU, 2-(7-Aza-1*H*-benzotriazole-1-yl)-1,1,3,3-tetramethyluronium hexafluorophosphate; HOBt, 1-hydroxybenzotriazole; HTS, high throughput screening; IGF1R, insulin-like growth factor-1 receptor; INSR, insulin receptor; JAK, janus kinase; NPM-ALK, nucleophosmin-ALK fusion protein; pALK IC<sub>50</sub>, inhibition of phosphorylation of ALK; pINSR IC<sub>50</sub>, inhibition of phosphorylation of INSR; PD, pharmacodynamic; PDB ID, Protein Data Bank identity number; PK, pharmacokinetics; POC, percent of control; SAR, structure–activity relationship; SFC, supercritical fluid chromatography; SRC, sarcoma kinase; TBAF, tetra *n*-butylammonium fluoride; TFA, trifluoroacetic acid; TIPS, triisopropylsilyl; TR-FRET, time-resolved-fluorescence resonance energy transfer; XDFG, amio acid residue which precedes the Asp-Phe-Gly sequence in ATP binding site

## ■ REFERENCES

- (1) George, R. E.; Sanda, T.; Hanna, M.; Froehling, S.; Luther, W., II; Zhang, J.; Ahn, Y.; Zhou, W.; London, W. B.; McGrady, P.; Xue, L.; Zozulya, S.; Gregor, V. E.; Webb, T. R.; Gray, N. S.; Gilliland, D. G.; Diller, L.; Greulich, H.; Morris, S. W.; Meyerson, M.; Look, A. Activating mutations in ALK provide a therapeutic target in neuroblastoma. *Nature* **2008**, *455*, 975–978.
- (2) Morris, S. W.; Kirstein, M. N.; Valentine, M. B.; Dittmer, K. G.; Shapiro, D. N.; Saltman, D. L.; Look, A. T. Fusion of a kinase gene, ALK, to a nucleolar protein gene, NPM, in non-Hodgkin's lymphoma. *Science* **1994**, *263*, 1281–1284.



(3) Soda, M.; Choi, Y. L.; Enomoto, M.; Takada, S.; Yamashita, Y.; Ishikawa, S.; Fujiwara, S.-I.; Watanabe, H.; Kurashina, K.; Hatanaka, H.; Bando, M.; Ohno, S.; Ishikawa, Y.; Aburatani, H.; Niki, T.; Sohara, Y.; Sugiyama, Y.; Mano, H. Identification of the transforming *EML4-ALK* fusion gene in non-small-cell lung cancer. *Nature* **2007**, *448*, 561–566 and references therein.

(4) <http://www.cancer.gov/cancertopics/druginfo/fda-crizotinib>; see also Shaw, A. T.; Yasothan, U.; Kirkpatrick, P.; crizotinib. *Nature Rev. Drug Discovery*, **2011**, *10*(12), 897–898, see also ref 9.

(5) (a) Bresler, S. C.; Wood, A. C.; Haglund, E. A.; Courtright, J.; Belcastro, L. T.; Plegaria, J. S.; Cole, K.; Toporovskaya, Y.; Zhao, H.; Carpenter, E. L.; Christensen, J. G.; Maris, J. M.; Lemmon, M. A.; Mossé, Y. P. Differential Inhibitor Sensitivity of Anaplastic Lymphoma Kinase Variants Found in Neuroblastoma. *Sci. Transl. Med.* **2011**, *108*(3), 108ra114, DOI: 10.1126/scitranslmed.3002950. (b) See also Sasaki, T.; Okuda, K.; Zheng, W.; Butrynski, J.; Capelletti, M.; Wang, L.; Gray, N. S.; Wilner, K.; Christensen, J. G.; Demetri, G.; Shapiro, G. I.; Rodig, S. J.; Eck, M. J.; Jänne, P. A. The neuroblastoma-associated F1174L ALK mutation causes resistance to an ALK kinase inhibitor in ALK-translocated cancers. *Cancer Res.* **2010**, *70* (24), 10038–43. (c) See also Choi, Y. L.; Soda, M.; Yamashita, Y.; Ueno, T.; Takashima, J.; Nakajima, T.; Yatabe, Y.; Takeuchi, K.; Hamada, T.; Haruta, H.; Ishikawa, Y.; Kimura, H.; Mitsudomi, T.; Tanio, Y.; Mano, H. *EML4-ALK* Mutations in Lung cancer that confer resistance to ALK inhibitors. *N. Engl. J. Med.* **2010**, *363* (18), 1734–1739. (d) See also Heuckmann, J. M.; Hoelzel, M.; Sos, M. L.; Heynck, S.; Balke-Want, H.; Koker, M.; Peifer, M.; Weiss, J.; Lovly, C. M.; Gruetter, C.; Rauh, D.; Pao, W.; Thomas, R. K. ALK Mutations Conferring Differential Resistance to Structurally Diverse ALK Inhibitors. *Clin. Cancer Res.* **2011**, *17* (23), 7394–7401.

(6) ALK, JAK2<sup>13</sup> and SRC are related in that they share a common downstream signaling pathway via Stat3. For details of the JAK kinase enzyme assays; see Laurie, B.; Schenkel, L. B.; Huang, X.; Cheng, A.; Deak, H. L.; Doherty, E.; Emkey, R.; Gu, Y.; Gunaydin, H.; Kim, J. L.; Lee, J.; Loberg, R.; Olivieri, P.; Pistillo, J.; Tang, J.; Wan, Q.; Wang, H.-L.; Wang, S.-W.; Wells, M. C.; Wu, B.; Yu, V.; Liu, L.; Geuns-Meyer, S. Discovery of Potent and Highly Selective Thienopyridine Janus Kinase 2 Inhibitors. *J. Med. Chem.* **2011**, *54* (24), 8440–8450.

(7) For details of the ALK kinase enzyme and cellular screens, see Drew, A. E.; Al-Assaad, S.; Yu, V.; Andrews, P.; Merkel, P.; Szilvassy, S.; Emkey, R.; Lewis, R.; Brake, R. L. Comparison of 2 Cell-Based Phosphoprotein Assays to Support Screening and Development of an ALK Inhibitor. *J. Biomol. Screening* **2011**, *16* (2), 164–173 Details of the IGF1R and SRC enzyme assays and INSR cellular assay are reported in the Supporting Information.

(8) IC<sub>50</sub> data from which these selectivity ratios are derived for the off-target kinases is included in the Supporting Information, Table S3, together with assay protocols (see also refs <sup>6</sup> and <sup>7</sup>). All IC<sub>50</sub> values are derived from 22 point dose–response curves and are reported as a mean (±) SD where two or more independent determinations were performed. ND = not determined.

(9) Cui, J. J.; Tran-Dube, M.; Shen, H.; Nambu, M.; Kung, P.-P.; Pairish, M.; Jia, L.; Meng, J.; Funk, L.; Botrous, I.; McTigue, M.; Grodsky, N.; Ryan, K.; Padrique, E.; Alton, G.; Timofeevski, S.; Yamazaki, S.; Li, Q.; Zou, H.; Christensen, J.; Mroczkowski, B.; Bender, S.; Kania, R. S.; Edwards, M. P. Structure Based Drug Design of Crizotinib (PF-02341066), a Potent and Selective Dual Inhibitor of Mesenchymal–Epithelial Transition Factor (c-MET) Kinase and Anaplastic Lymphoma Kinase (ALK). *J. Med. Chem.* **2011**, *54* (18), 6342–6363.

(10) ((a)) There is evidence of a close association between the benzimidazole nitrogen and the backbone carbonyl of Met1199 in all of the co-crystal structures that we have obtained for this class of ALK inhibitors. For compound **36** (Figure 3), the N-to-O distance is measured at 2.9 Å, which is consistent with an intermolecular hydrogen bond between these two centers. The interatomic distance between the benzoyl carbonyl oxygen of the inhibitor and the backbone NH of Met1199 measures 3.0 Å in this structure. These interatomic distances are compatible with this class of compounds

adopting an exocyclic acylimine tautomer, which is best able to satisfy the observed hydrogen-bonding pattern. Riether, D.; Zindell, R.; Kowalski, J. A.; Cook, B. N.; Bentzien, J.; De Lombaert, S.; Thomson, D.; Kugler, S. Z., Jr.; Skow, D.; Martin, L. S.; Raymond, E. L.; Khine, H. H.; O'Shea, K.; Woska, J. R., Jr.; Jeanfavre, D.; Sellati, R.; Ralph, K. L. M.; Ahlberg, J.; Labissiere, G.; Kashem, M. A.; Pullen, S. S.; Takahashi, H. 5-Aminomethylbenzimidazoles as potent ITK antagonists. *Bioorg. Med. Chem. Lett.* **2009**, *19*, 1588–1591. ((b)) See also Cook, B. N.; Bentzien, J.; White, A.; Nemoto, P. A.; Wang, J.; Man, C. C.; Soleymanzadeh, F.; Khine, H. H.; Kashem, M. A.; Kugler, S. Z., Jr.; Wolak, J. P.; Roth, G. P.; De Lombaert, S.; Pullen, S. S.; Takahashi, H. Discovery of potent inhibitors of interleukin-2 inducible T-cell kinase (ITK) through structure-based drug design. *Bioorg. Med. Chem. Lett.* **2009**, *19*, 773–777. ((c)) For a discussion of acyliminobenzimidazole tautomerism, see Snow, R. J.; Abeywardane, A.; Campbell, S.; Lord, J.; Kashem, M. A.; Khine, H. H.; King, J.; Kowalski, J. A.; Pullen, S. S.; Roma, T.; Roth, G. P.; Sarko, C. R.; Wilson, N. S.; Winters, M. P.; Wolak, J. P.; Cywin, C. L. Hit-to-lead studies on benzimidazole inhibitors of ITK: discovery of a novel class of kinase inhibitors. *Bioorg. Med. Chem. Lett.* **2007**, *17*, 3660–3665. ((d)) See also Wang, Z.; Liu, J.; Sudom, S.; Ayres, M.; Li, S.; Wesche, H.; Powers, J. P.; Walker, N. P. C. Crystal Structures of IRAK-4 Kinase in Complex with Inhibitors: A Serine/Threonine Kinase with Tyrosine as a Gatekeeper. *Structure* **2006**, *14*, 1835–1844.

(11) Data collection and refinement statistics are included in the Supporting Information, Table S4, along with crystallographic experimental procedures. The cocrystal structures of **1** and **2** in ALK have PDB codes 4FOB and 4FOC, respectively; **3**, PF-02341066, hydrogen-bonds to the linker region of ALK through its pyridine nitrogen atom and the adjacent amine. The pyrazole ring and solubilizing group face solvent and the O-linked benzyl ring sits in the lipophilic pocket defined largely by Leu1256, Gly1269 (the X-DFG residue), and the backbone atoms of Arg1253/Asn1254 (PDB code 2XP2).

(12) SAR of the sulfonamide side chain of **1** or ester moiety of **2** indicated that the cost of not occupying this lipophilic pocket amounted to an order of magnitude loss in binding affinity. Unpublished observations.

(13) Activity against JAK1, **2**, and **3** and TYK2 were routinely monitored,<sup>6</sup> and selectivity over JAK2 was the highest hurdle for this structural class. Selected data for compounds **14**, **1**, and **36**, typical for this class, is included in the Supporting Information, Table S1.

(14) Bode, C. M.; Cheng, A. C.; Choquette, D.; Lewis, Richard T.; Potashman, M. H.; Romero, K.; Stellwagen, J. C.; Whittington, D. A. Benzimidazole and azabenzimidazole compounds that inhibit anaplastic lymphoma kinase. *PCT Int. Appl. WO 2012018668*, 2012.

(15) Point changes with respect to the residues which flank the benzamide moiety are summarized for closely related kinases in the Supporting Information in Table S2.

(16) Microsomal turnover protocol: 0.5 mg/mL of protein, 1 μM substrate, 1 mM NADPH, 30 min incubation, pH 7.4, and 37 °C.

(17) Screen was performed by KINOMEScan, a division of DiscoveRx, 11180 Roselle Street, San Diego, CA 92121 USA; <http://kinomescan.com/>.

(18) See Supporting Information for assay protocol.

(19) Screen was performed by Carna Biosciences. <https://www.carnabio.com/english/product/search.cgi?mode=profiling>.

(20) Douglas C. Saffran unpublished results. See Figure S1 in the Supporting Information for body weight data associated with the Karpas299 xenograft study.

(21) Yohannes Teffera unpublished results.

(22) Details of additional studies will be reported elsewhere. In March 2011, Tesaro, Inc. signed an agreement with Amgen granting Tesaro exclusive worldwide rights for the development, manufacture, commercialization, and distribution of small molecule inhibitors of ALK. For more information, please contact Dr. Mary Lynne Hedley: [MLHedley@tesarobio.com](mailto:MLHedley@tesarobio.com)

(23) Allen, J. R.; Bourbeau, M. P.; Chen, N.; He, E.; Kunz, R.; Rumpf, S. Pyrazine compounds as phosphodiesterase 10 inhibitors

and their preparation and use in the treatment of diseases. WO 2010/057121, 2010.

(24) Allen, J. R.; Chen, N.; Falsey, J. R.; Frohn, M.; Harrington, P.; He, E.; Kaller, M. R.; Kunz, R.; Mercede, S. J.; Nguyen, T. T.; Pickrell, A. J.; Reichelt, A.; Rumfelt, S.; Rzasa, R. M.; Sham, K.; Siegmund, A. C.; Tegley, C. M.; Yao, G. Aminopyridine and carboxypyridine compounds as phosphodiesterase 10 inhibitors. U.S. Patent US 2010/0160280, 2010.

(25) Castanedo, G.; Chan, B.; Goldstein, D. M.; Kondru, R. K.; Lucas, M. C.; Palmer, W. S.; Price, S.; Safina, B.; Savy, P. P. A.; Seward, E. M.; Sutherlin, D. P.; Sweeney, Z. K. Preparation of bicyclic pyrimidines as selective inhibitors of the p110 delta isoform of PI3K for treating inflammation, immune diseases, and cancers. WO 2010/138589, 2010.